Author's personal copy

ratio was compared, kaolin intake was significantly decreased by CP-99,994 (60 mg/kg) compared with saline ($p<0.05$), CP-99,994 (30 mg/kg) ($p<0.05$), and enantiomer CP-100,263 (60 mg/kg) ($p<0.01$) as shown in Fig. 2A. In contrast, food intake after hypergravity load was neither affected by saline, CP-99,994 (30 mg/kg or 60 mg/kg), nor by enantiomer CP-100,263 (60 mg/kg) as shown in Fig. 2B.

2.2. *Preprotachykinin and NK-1 receptor mRNA expression*

Fig. 3 shows the changes in preprotachykinin mRNA expression in each subnucleus of amygdala and solitary tract nucleus of animals exposed to 2G hypergravity for 3 h. Accordingly, preprotachykinin mRNA expression was significantly increased in basolateral nucleus of the amygdala (Fig. 3B) and solitary tract nucleus (Fig. 3D) compared with control animals. However, 2G hypergravity load did not influence the expression of preprotachykinin mRNA in the central nucleus (Fig. 3A) and medial nucleus of amygdala (Fig. 3C).

Fig. 4 shows the effects of 2G hypergravity load for 3 h on NK-1 receptor mRNA expression in each subnucleus of the amygdala and solitary tract nucleus. No change in NK-1 receptor mRNA expression was noticed in both areas.

3. Discussion

Rats cannot vomit but show pica behavior, that is eating non-nutritive substances such as kaolin, which is the analog to emetic response in rats (Takeda et al., 1993). As shown in Fig. 1, there was a trend to increasing kaolin intake by 2G hypergravity load day by day. In our previous studies, kaolin intake was increased 2 days after the start of hypergravity reaching a peak 3–6 days afterward. This phenomenon is consistent with previous reports (Morita et al., 1990) and suggests that animals have to learn that kaolin was effective for resulting emesis following provocative motion stimuli within the early stage of hypergravity exposure (1–2 days) followed by a peak of kaolin intake (3–6 days). Then, the intake gradually declined and no significant kaolin intake was observed about 10–12 days after the start of hypergravity, even when exposed to another hypergravity, indicating a possible adaptation to this environment (unpublished observation). Therefore, we examined the effects of any drug administration on kaolin intake 3 or 4 days after the start of the hypergravity load. And, as shown in Fig. 1, NK-1 receptor antagonist CP-99,994 at a dose of 60 mg/kg effectively suppressed the kaolin intake induced by 2G hypergravity compared with animals injected with saline or a smaller dose of CP-99,994 (30 mg/kg). However, this effect was not different from its enantiomer CP-100,263. Indeed, kaolin intake at Day 1 and Day 2 in animals injected with CP-100,263 was slightly smaller compared with other groups, but the difference was not statistically significant. Given the difficulty to compare the drug effects on Day 3 and Day 4 with other groups, we evaluated the drug effects by examining the ratio before and after drug administration: post-treatment kaolin intake/pre-treatment kaolin intake. As shown in Fig. 2A, kaolin intake ratio (Day 3+4/Day 1+2) was significantly lower in animals injected with CP-99,994 (60 mg/kg) compared with those with enantiomer CP-100,263 (60 mg/kg), smaller dose of CP-99,994 (30 mg/kg) or saline, indicating that the effects of CP-99,994 on hypergravity-induced motion sickness were dose-dependent and enantioselective. Food intake ratio (Day 3+4/Day 1+2) after hypergravity

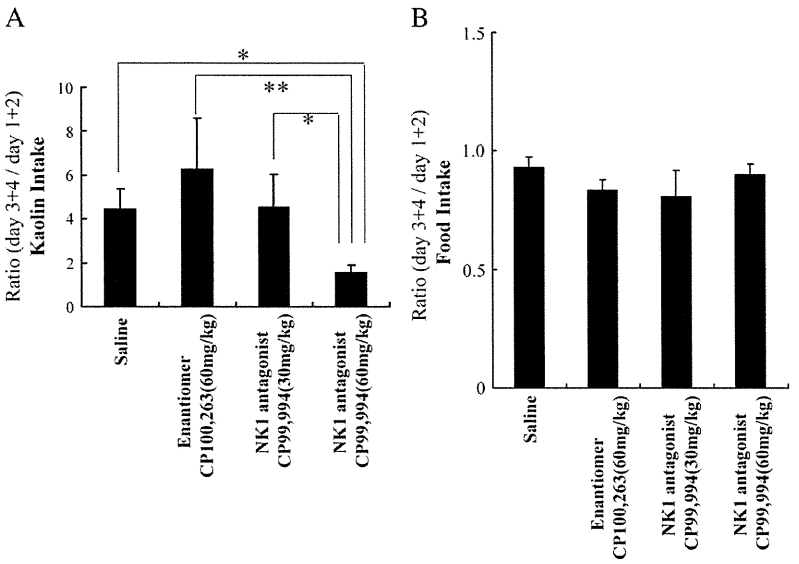

Fig. 2 – Day 3+4/Day 1+2 ratio of kaolin (A) and food (B) intake after drug administration. Panel A shows that kaolin intake induced by hypergravity load was significantly decreased by CP-99,994 (60 mg/kg) compared with saline ($p<0.05$), CP-99,994 (30 mg/kg) ($p<0.05$), and enantiomer CP-100,263 (60 mg/kg) ($p<0.01$). Panel B shows that food intake after hypergravity load was neither affected by saline, CP-99,994 (30 mg/kg or 60 mg/kg), nor enantiomer CP-100,263 (60 mg/kg).

Author's personal copy

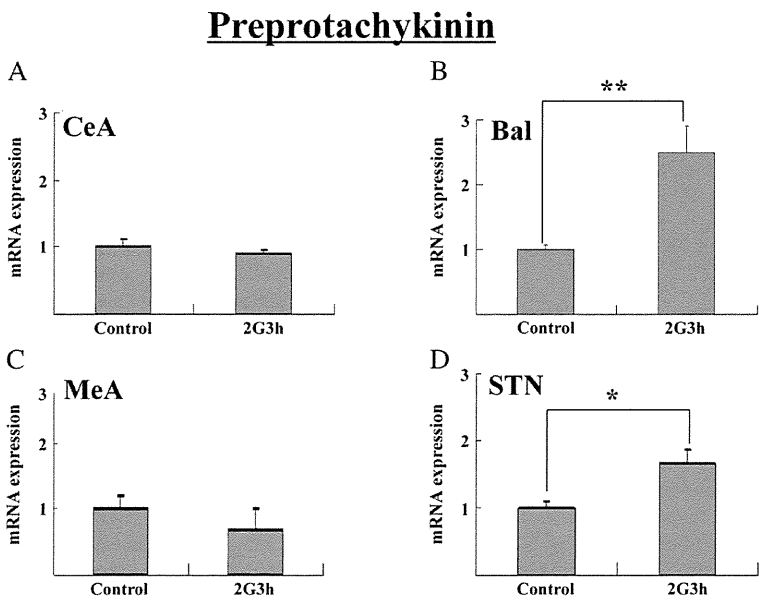

Fig. 3 – Changes in preprotachykinin mRNA expression in each subnucleus of amygdala and solitary tract nucleus of animals exposed to 2G hypergravity for 3 h. Preprotachykinin mRNA expression was significantly increased in basolateral nucleus of amygdala (B) and solitary tract nucleus (D) compared with control animals. In central nucleus (A) and medial nucleus (C) of amygdala, preprotachykinin mRNA expression was not changed by 2G hypergravity load.

load was not affected by any drug administration as shown in Fig. 2B, suggesting that kaolin intake suppression induced by CP-99,994 (60 mg/kg) can be considered specific. Indeed, kaolin intake at Day 5 in CP-99,994 (60 mg/kg) group was significantly higher than that at Day 4, suggesting that this is a real drug effect and not merely adaptation to the 2G exposure, since kaolin intake increased as soon as the drug was stopped. This is the first report indicating that NK-1 receptor antagonist CP-99,994 was effective in preventing emesis induced by provocative motion stimuli in rats. In other species, resinferatoxin, a compound

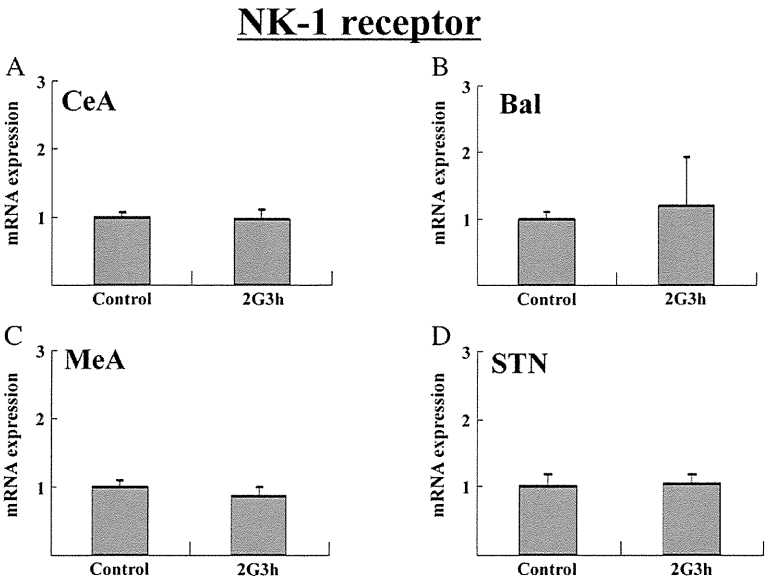

Fig. 4 – Changes in NK-1 receptor mRNA expression in each subnucleus of amygdala and solitary tract nucleus of animals exposed to 2G hypergravity for 3 h. NK-1 receptor mRNA expression was not changed by 2G hypergravity load for 3 h in all subnuclei of amygdala and solitary tract nucleus.

Author's personal copy

that depletes substance P as well as the selective NK-1 receptor antagonist (CP-99,994 or maropitant) were shown to have anti-emetic properties in cats, dogs, suncus, and ferrets (Andrews and Bhandari, 1993; Andrews et al., 2000; Hickman et al., 2008; Lucot et al., 1997; Rudd et al., 1999; Watson et al., 1995). Taken together, the above data suggest that substance P and its receptor, NK-1 play an important role in the development of motion sickness in rats.

Microinjection of substance P into the brain stem elicits an immediate emetic response (Gardner et al., 1994). Moreover, previous reports demonstrated that NK-1 antagonists had a broad anti-emetic property against various emetic substances including nicotine, copper sulfate, xylazine and motion, suggesting that NK-1 antagonists would block the final common pathways of emesis such as brain stem emetic center (Hickman et al., 2008; Rudd et al., 1999; Rupniak and Kramer 1999). In the present study, mRNA expression of preprotachykinin, a precursor of substance P, was increased in not only the solitary tract nucleus in the brain stem but also in the basolateral nucleus of amygdala by 2G hypergravity load. We previously reported that 2G hypergravity load increased Fos protein expression in the central nucleus of amygdala and solitary tract nucleus (Nakagawa et al., 2003). The subnucleus activated by 2G hypergravity was different between the previous and the present study. However, the present results taken together, suggest that 2G hypergravity load activated the substance P neuronal system in amygdala as well as in the brain stem, leading to the development of motion sickness. In future studies, changes in protein expression of substance P in subnuclei of the amygdala should be investigated.

As discussed in the above paragraph, 2G hypergravity load activated the substance P neuronal system in the amygdala, but did not affect the mRNA expression of NK-1 receptor in all the subnuclei of the amygdala and solitary tract nucleus. Another neuronal system involved in neural mechanisms of motion sickness might be the increase of histamine release in the hypothalamus by vestibular stimulation including 2G hypergravity load as well as electric or caloric stimulation of the inner ear as revealed by in vivo microdialysis technique (Horii et al., 1993; Uno et al., 1997). As a post-synaptic event, the gene expression of post-synaptic histamine H1 receptors in the brain stem and hypothalamus was increased after 4 h-exposure to 2G hypergravity (Sato et al., 2009). This up-regulation was supposed to be involved in the characteristic time course of motion sickness symptoms that develop gradually and then progress rapidly. In contrast to the histaminergic receptors, post-synaptic NK-1 receptors were not increased by 2G hypergravity load in the present study. Because the stimulation period was different between experiments (3 h vs. 4 h), the effects of 2G hypergravity load on receptor expression in the brain might also be different between the histaminergic and substance P neuronal systems. These differences in response to provocative motion stimuli between the two neuronal systems might be related to different roles played by these systems in the development of motion sickness: the histaminergic neurons being involved in the final step of vomiting, whereas substance P neurons might be related to the convergence and comparison of sensory inputs in the development of motion sickness.

In conclusion, hypergravity-induced motion sickness was inhibited by NK-1 antagonist in a dose-dependent and enantioselective manners. Preprotachykinin mRNA expression was increased in both the basolateral nucleus of the amygdala and solitary tract nucleus after 2G hypergravity load, whereas NK-1 receptor mRNA expression was not changed in all subnuclei of amygdala and solitary tract nucleus. It is suggested that 2G hypergravity load activated the substance P neuronal system in the amygdala as well as in the brain stem, indicating the involvement of substance P in the development of motion sickness.

4. Experimental procedures

4.1. *Animals and experimental protocol*

All animal experiments were conducted under approval of the Animal Care Committee of Osaka University Graduate School of Medicine. Male Wistar rats (Japan SLC, Shizuoka, Japan) weighing 180–200 g were used. Animals were exposed to 2G hypergravity in a centrifuge device (Takeda et al., 1996) and their emesis induced by 2G hypergravity load was evaluated by pica behavior, which is eating non-nutritive substances such as kaolin (Takeda et al., 1993). Animals were individually housed in home cages with free access to food, kaolin and water in a room with a 12 h light/12 h dark cycle (light from 8:00 to 20:00) for at least 3 days before the start of the experiment to avoid stress associated with isolation and/or transportation. Following these initial adaptation days, they were housed in home cages without hypergravity load for three days, during which food and kaolin consumption were measured. Then, animals were exposed to 2G hypergravity load for 2 h (18:00–20:00)/day for five days. Rats were, then, randomly divided into 4 groups on Day 2 and administered intraperitoneal NK-1 antagonist CP-99,994 (60 mg/kg, n=6), CP-99,994 (30 mg/kg, n=5), inactive enantiomer of NK-1 antagonist CP-100,263 (60 mg/kg, n=5) and saline (3 ml/kg, n=6), respectively. On Day 3 and Day 4, drugs or saline were administrated 30 min before the hypergravity load. Gene expression of NK-1 receptors and preprotachykinin in subnuclei of the amygdala and solitary tract nucleus was evaluated using quantitative real-time PCR methods coupled with micropunch technique in another group of 29 rats. In this group, 16 rats were exposed to 2G hypergravity for 3 h, whereas 13 with no hypergravity exposure served as controls, but were placed near the centrifuge device for the same period.

4.2. *Hypergravity load*

Rats were exposed to 2G hypergravity in an animal cage, which was suspended with swing arms connected to a turntable of the centrifuge device (Takeda et al., 1996). The turntable was driven by a servo-controlled torque motor and rotated at a constant rate (336°/s, 56 rpm), loading the animal with the vector sum of gravity linear acceleration (1G) and rotational centrifugal linear acceleration (1.73G) vectors. This achieved a resultant linear acceleration of 2G acting on the animal along its dorso-ventral axis. This constant gravito-inertial force was expected to induce mainly saccular stimulation. In addition, since animals could

Author's personal copy

move freely in the cage during centrifugation, they were also subjected to intermittent and variable Coriolis acceleration, which is dependent on animals' motion acting mainly on the utricle (Gustave Dit Duflo et al., 2000).

4.3. *Kaolin consumption*

Pharmaceutical grade kaolin (hydrated aluminum silicate, Katayama Pharmaceutical Co., Japan) was mixed with 1% Arabic gum in distilled water to form a column of the same shape as that of normal food pellets, which were placed in a container next to the food in home cages. Consumption of kaolin and food for 24 h was determined by measuring its weight to the nearest 0.1 g at 19:00 h every day. Spilt kaolin was collected and weighed to obtain correct values for kaolin consumption.

4.4. *Gene expression of NK-1 receptors and preprotachykin*

Effects of 2G hypergravity load for 3 h on mRNA expression of NK-1 receptor and preprotachykinin in the subnuclei of the amygdala (central nucleus, CeA; basolateral nucleus, Bal; medial nucleus, MeA) and solitary tract nucleus were measured using quantitative real-time PCR methods. Control animals were placed in the animal cages beside the centrifuge device for the same period but were not exposed to hypergravity.

Just after exposure to hypergravity, animals were sacrificed by decapitation under overdose anesthesia with pentobarbital (60 mg/kg). Brains were carefully removed from the skull and cooled in iced saline for 1 min. Then, coronal sections of the brain block were cut at 200 μm thickness on a cryostat. Each slice was mounted on a slide glass. Central, basolateral and medial nuclei of the amygdala and solitary tract nucleus including the area postrema were, then, separately dissected on a chilled aluminum plate with blunted 22 gauge needle using a micropunch technique (Pi and Grattan, 1998). Fig. 5 shows a representative slice from which subnuclei of the amygdala and solitary tract nucleus were punched out.

Detailed procedures for real-time PCR have been described elsewhere (Horii et al., 2001, 2002, 2003, 2004). Tissue samples were homogenized in a sonicator coupled with a cup-horn attachment (Sonics & Materials, Danbury, CT, USA), and total RNA was extracted using an RNeasy Mini Kit (Qiagen, Tokyo, Japan). The RNA sample was treated with RNase-free DNase I (Boehringer Mannheim, Mannheim, Germany) to remove any contaminating genomic DNA before RT. DNase I-treated RNA sample was reverse transcribed using the SuperScriptTM First-Strand Synthesis System for RT-PCR Kit with oligo (dT) 12–18 primer (Invitrogen, Carlsbad, California, USA). Negative control samples without reverse transcription were also forwarded to PCR to confirm that no genomic DNA contamination occurred.

PCR reactions were performed in the presence of three sequence-specific oligonucleotides. Two of them were forward and reverse primers for PCR. The third oligonucleotide (TaqMan probe) was designed to hybridize to the portion of the PCR product between the forward and reverse primer. TaqMan probe was labeled with a fluorescent reporter dye and a quenching dye at the 5′- and 3′ end, respectively. The fluorescent emission of the reporter dye was neutralized

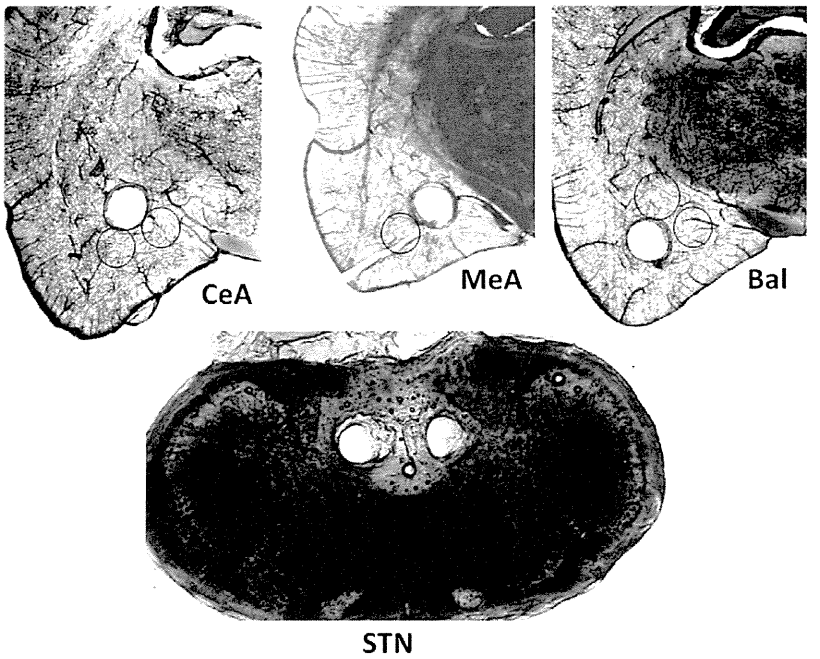

Fig. 5 – Photomicrograph of representative slices from which subnuclei of amygdala and solitary tract nucleus were punched out. Central (Ce), medial (Me), and basolateral (Bal) nucleus of the amygdala and solitary tract nucleus (STN) were selectively punched out.

Author's personal copy

with a quenching dye, when the TaqMan probe was hybridized to the PCR product. During PCR amplification, Taq DNA polymerase cleaved the TaqMan probe into fragments by its 5′ to 3′ endonucleolytic activity and thus the reporter dye was separated from the quenching dye. This resulted in an increase in fluorescence emission, which was proportional to the amount of amplification of the molecule. The number of PCR cycles when the fluorescence intensity exceeded a predetermined threshold was measured during PCR. Quantification of the initial amount of template molecules relied on this number of PCR cycles, which is termed the cycle of threshold (CT). The difference in the initial amount of total RNA between the samples was normalized in every assay using a glyceraldehyde-3-phosphate dehydrogenase (GAPDH) housekeeping gene expression as an internal standard.

Seventy five nanograms of cDNA was reacted in a total volume of 30 μl with a TaqMan Universal PCR Master Mix (Perkin Elmer, USA). The final concentration of TaqMan probe for the target molecules and GAPDH was 200 nM, and that of the primers for the target molecules and GAPDH was 400 nM. PCR thermal cycle conditions were as follows: 50 °C for 2 min, 95 °C for 10 min for an initial denaturing, 40 cycles of heating at 95 °C for 15 s for denaturing, and 60 °C for 1 min for annealing and extension. PCR primers and TaqMan probes for the target molecules were commercially synthesized by Sawady Technology (Japan) and Perkin Elmer (USA), respectively. PCR primers and TaqMan probe for GAPDH were purchased from Perkin Elmer (TaqMan Rodent GAPDH Control Reagents). Sequences and fluorescent dye of these oligonucleotides specific for the target molecules and GAPDH are as follows: Preprotachykinin (Acc. No. M34183) forward primer 5′-TGA CCA AAT CAA GGA GGC AAT-3′, reverse primer 5′-GGG TCT TCG GGC GAT TCT-3′, TaqMan probe 5′-FAM-CCG GAG CCC TTT GAG CAT CTT CTT C-TAMRA-3′, NK-1 Receptor (Acc. No. M64263) forward primer 5′-GGC CTT TCC ACA AGG CTA CTA CT-3′, reverse primer 5′-GTC ACG CAG ATG TGG TAC GCT-3′, TaqMan probe 5′-FAM-CAC TCG ATC ATG CAC ACG ACT CTG CTG-TAMRA-3′, GAPDH forward primer 5′-TGC ACC ACC AAC TGC TTA G-3′, reverse primer 5′-GGA TGC AGG GAT GAT GTT C-3′, TaqMan probe 5′-VIC-CAG AAG ACT GTG GAT GGC CCC TC-TAMRA-3′.

cDNA from one of the control animals was used as standard samples for constructing standard curves. The standard cDNA sample was diluted in four steps from three times to 3^4 times. Then, standard curves plotting the relative concentration of cDNA and CT values were constructed for both GAPDH and the target molecules for every PCR assay. From the standard curves, the relative concentration of the target molecules and GAPDH in the samples was calculated based on the CT values of each sample. GAPDH was amplified with target molecule in the same PCR plate in every PCR. Ratio of relative concentration of each target molecule to GAPDH (target molecule/GAPDH) was calculated. This value indicated the expression of the target molecule in each sample compared with the standard sample, which had been normalized by GAPDH expression.

4.5. Statistics

Differences in kaolin and food consumption between the groups (CP-99,994 at a dose of 60 mg/kg, CP-99,994 at a dose of 30 mg/kg, enantiomer CP-100,263 at a dose of 60 mg/kg, and saline at a dose of 3 ml/kg) were tested with a 2-way ANOVA with repeated measure followed by Scheffe's post-hoc test. Mann–Whitney's U-test was used for testing differences in gene expression between the hypergravity-loaded animals and control animals. P-values under 0.05 were considered significant.

Acknowledgments

This study was partly supported by grants-in-aid for scientific research from the Ministry of Education, Culture, Sports, Science and Technology of Japan for AH. We thank Dr. Kalubi Bukasa for the critical reading of the manuscript, Dr. Takefumi Kamakura for the preparation of histology, and Dr. Yasuhiro Osaki for creating figures.

REFERENCES

Andrews, P.L., Bhandari, P., 1993. Resinferatoxin, an ultrapotent capsaicin analogue, has anti-emetic properties in the ferret. Neuropharmacology 32, 799–806.

Andrews, P.L., Okada, F., Woods, A.J., Hagiwara, H., Kakaimoto, S., Toyoda, M., Matsuki, N., 2000. The emetic and anti-emetic effects of the capsaicin analogue resiniferatoxin in *Suncus murinus*, the house musk shrew. Br. J. Pharmacol. 130, 1247–1254.

Brizzee, K.R., 1990. The central nervous connections involved in motion induced emesis. In: Crampton, G.H. (Ed.), Motion and Space Sickness. CRC Press, Boca Raton, FL, USA, pp. 9–28.

Gallagher, M., Chiba, A.A., 1996. The amygdala and emotion. Curr. Opin. Neurobiol. 6, 221–227.

Gardner, C.J., Bountra, C., Bunce, K.T., Dale, T.J., Jordan, C.C., Twissell, D.J., Ward, P., 1994. Anti-emetic activity of neurokinin NK receptor antagonists is mediated centrally in the ferret. Br. J. Pharmacol. 112, 516.

Gustave Dit Duflo, S., Gestreau, C., Lacour, M., 2000. Fos expression in the rat brain after exposure to gravito-inertial force changes. Brain Res. 861, 333–344.

Hickman, M.A., Cox, S.R., Mahabir, S., Miskell, C., Lin, J., Bunger, A., McCall, R.B., 2008. Safety, pharmacokinetics and use of the novel NK-1 receptor antagonist maropitant (Cerenia) for the prevention of emesis and motion sickness in cats. J. Vet. Pharmacol. Ther. 31, 220–229.

Horii, A., Takeda, N., Matsunaga, T., Yamatodani, A., Mochizuki, T., Okakura-Mochizuki, K., Wada, H., 1993. Effect of unilateral vestibular stimulation on histamine release from the hypothalamus of rats in vivo. J. Neurophysiol. 70, 1822–1826.

Horii, A., Smith, P.F., Darlington, C.L., 2001. Quantitative changes in gene expression of glutamate receptor subunits/subtypes in the vestibular nucleus, inferior olive and flocculus before and following unilateral labyrinthectomy in the rat: real-time quantitative PCR method. Exp. Brain Res. 139, 188–200.

Horii, A., Smith, P.F., Darlington, C.L., 2002. Application of real-time quantitative polymerase chain reaction to quantification of glutamate receptor gene expression in the vestibular brainstem and cerebellum. Brain Res. Protoc. 9, 77–83.

Horii, A., Kitahara, T., Smith, P.F., Darlington, C.L., Masumura, C., Kubo, T., 2003. Effects of unilateral labyrinthectomy on GAD, GAT1 and GABA receptor gene expression in the rat vestibular nucleus. Neuroreport 14, 2359–2363.

Author's personal copy

Horii, A., Masumura, C., Smith, P.F., Darlington, C.L., Kitahara, T., Uno, A., Mitani, K., Kubo, T., 2004. Microarray analysis of gene expression in the rat vestibular nucleus complex following unilateral vestibular deafferentation. J. Neurochem. 91, 975–982.

Inagaki, S., Sakanaka, M., Shiosaka, S., Senba, E., Takatsuki, K., Takagi, H., Kawai, Y., Minagawa, H., Tohyama, M., 1982. Ontogeny of substance P-containing neuron system of the rat: immunohistochemical analysis—I. Forebrain and upper brain stem. Neuroscience 7, 251–277.

Lucot, J.B., Obach, R.S., McLean, S., Watson, J.W., 1997. The effect of CP-99994 on the responses to provocative motion in the cat. Br. J. Pharmacol. 120, 116–120.

Mantyh, P.W., Hunt, S.P., Maggio, J.E., 1984. Substance P receptors: localization by light microscopic autoradiography in rat brain using [3H] SP as the radioligand. Brain Res. 307, 147–165.

Miller, A.D., Nonaka, S., Jakus, J., 1994. Brain areas essential or non-essential for emesis. Brain Res. 647, 255–264.

Morita, M., Takeda, N., Hasegawa, S., Yamatodani, A., Wada, H., Sakai, S., Kubo, T., Matsunaga, T., 1990. Effects of anti-cholinergic and cholinergic drugs on habituation to motion in rats. Acta Otolaryngol. 110, 196–202.

Nakagawa, A., Uno, A., Horii, A., Kitahara, T., Kawamoto, M., Uno, Y., Fukushima, M., Nishiike, S., Takeda, N., Kubo, T., 2003. Fos induction in the amygdala by vestibular information during hypergravity stimulation. Brain Res. 986, 114–123.

Ono, T., Nishijo, H., Uwano, T., 1995. Amygdala role in conditioned associative learning. Prog. Neurobiol. 46, 401–422.

Pi, X.J., Grattan, D.R., 1998. Differential expression of the two forms of prolactin receptor mRNA within microdissected hypothalamic nuclei of the rat. Mol. Brain Res. 59, 1–12.

Reason, J.T., 1978. Motion sickness adaptation: a neural mismatch model. J. R. Soc. Med. 71, 819–829.

Rudd, J.A., Ngan, M.P., Wai, M.K., 1999. Inhibition of emesis by tachykinin NK1 receptor antagonists in *Suncus murinus* (house musk shrew). Eur. J. Pharmacol. 366, 243–252.

Rupniak, N.M., Kramer, M.S., 1999. Discovery of the antidepressant and anti-emetic efficacy of substance P receptor (NK1) antagonists. Trends Pharmacol. Sci. 20, 485–490.

Sakanaka, M., Inagaki, S., Shiosaka, S., Senba, E., Takagi, H., Takatsuki, K., Kawai, Y., Iida, H., Hara, Y., Tohyama, M., 1982. Ontogeny of substance P-containing neuron system of the rat: immunohistochemical analysis—II. Lower brain stem. Neuroscience 7, 1097–1126.

Sato, G., Uno, A., Horii, A., Umehara, H., Kitamura, Y., Sekine, K., Tamura, K., Fukui, H., Takeda, N., 2009. Effects of hypergravity on histamine H1 receptor mRNA expression in hypothalamus and brainstem of rats: implications for development of motion sickness. Acta Otolaryngol. 129, 45–51.

Takeda, N., Hasegawa, S., Morita, M., Matsunaga, T., 1993. Pica in rats is analogous to emesis: an animal model in emesis research. Pharmacol. Biochem. Behav. 45, 817–821.

Takeda, N., Horii, A., Uno, A., Morita, M., Mochizuki, T., Yamatodani, A., Kubo, T., 1996. A ground-based animal model of space adaptation syndrome. J. Vestib. Res. 6, 403–409.

Uno, A., Takeda, N., Horii, A., Morita, M., Yamamoto, Y., Yamatodani, A., Kubo, T., 1997. Histamine release from hypothalamus induced by gravity change in rats and space motion sickness. Physiol. Behav. 61, 883–887.

Uno, A., Takeda, N., Horii, A., Sakata, Y., Yamatodani, A., Kubo, T., 2000. Effects of amygdala or hippocampus lesion on hypergravity-induced motion sickness in rats. Acta Otolaryngol. 120, 860–865.

Watson, J.W., Gonsalves, S.F., Fossa, A.A., McLean, S., Seeger, T., Obach, S., Andrews, P.L., 1995. The anti-emetic effects of CP-99,994 in the ferret and the dog: role of the NK1 receptor. Br. J. Pharmacol. 115, 84–94.

Provided for non-commercial research and education use.
Not for reproduction, distribution or commercial use.

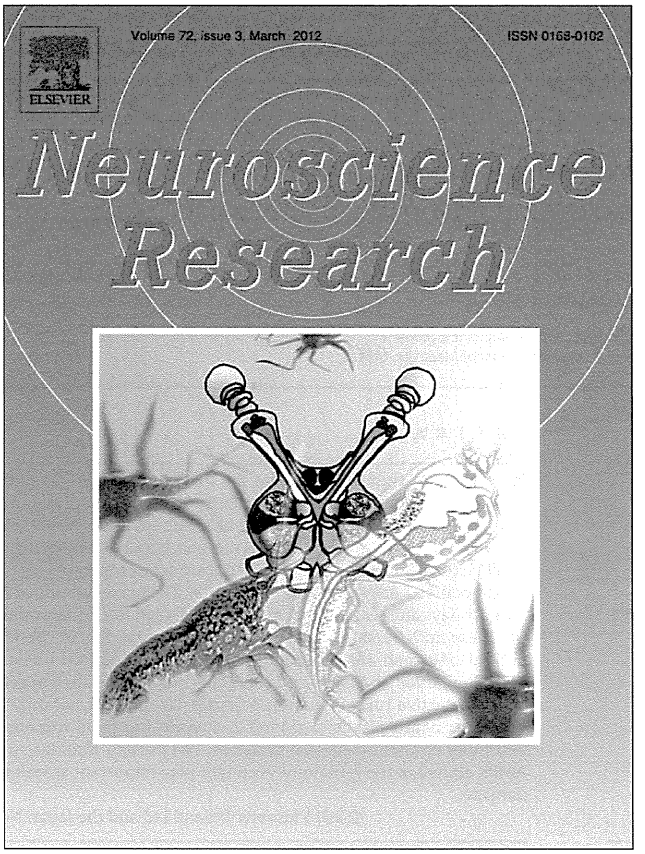

This article appeared in a journal published by Elsevier. The attached copy is furnished to the author for internal non-commercial research and education use, including for instruction at the authors institution and sharing with colleagues.

Other uses, including reproduction and distribution, or selling or licensing copies, or posting to personal, institutional or third party websites are prohibited.

In most cases authors are permitted to post their version of the article (e.g. in Word or Tex form) to their personal website or institutional repository. Authors requiring further information regarding Elsevier's archiving and manuscript policies are encouraged to visit:

http://www.elsevier.com/copyright

Author's personal copy

Neuroscience Research 72 (2012) 221–226

Contents lists available at SciVerse ScienceDirect

Neuroscience Research

journal homepage: www.elsevier.com/locate/neures

Changes in beta-2 adrenergic receptor and AMP-activated protein kinase alpha-2 subunit in the rat vestibular nerve after labyrinthectomy

Tadashi Kitahara[a,b,*], Arata Horii[a], Atsuhiko Uno[a], Takao Imai[a], Suzuyo Okazaki[a], Takefumi Kamakura[a], Yasumitsu Takimoto[a], Hidenori Inohara[a]

[a] Department of Otolaryngology, Osaka University, School of Medicine, Japan
[b] Department of Otolaryngology, University of Pittsburgh, School of Medicine, USA

ARTICLE INFO

Article history:
Received 9 August 2011
Received in revised form
18 November 2011
Accepted 21 November 2011
Available online 8 December 2011

Keywords:
Unilateral labyrinthectomy
Vestibular ganglion
Adrenergic receptor
Thermogenic signaling
Neural plasticity
AMP-activated protein kinase
Oxidative stress
Cell survival

ABSTRACT

In the present study, to elucidate the role of vestibular ganglion (VG) after the unilateral labyrinthine damage, we examined quantitative changes in mRNA expression of beta-adrenergic receptors (bARs) and AMP-activated protein kinase alpha catalytic subunits (aAMPKs) in VG after unilateral labyrinthectomy (UL) in rats. Using the real-time PCR method, beta2 AR mRNA expression in bilateral VG and AMPK alpha2 mRNA expression in the ipsilateral VG were significantly up-regulated with the maximum increase at the postoperative 7 day and 1 day, respectively. The up-regulation of beta2 AR in bilateral VG was long-lasting until 28 days after UL and that of AMPK alpha2 in the ipsilateral VG was just transient within 7 days after UL. These mRNA changes were supported by immunohistochemical data. According to previous reports, both of bARs and aAMPKs could regulate mitochondrial uncoupling protein (UCP) mRNA expression in several kinds of tissues and therefore might have thermogenic neurotransmission and antioxidant neuroprotective roles in neuronal tissues. UL requires not only long-lasting response of VG for central vestibular neuro-plasticity around 2–4 weeks but rapid response of VG against apoptosis of peripheral vestibular epithelia-neuronal synapses. The present findings suggest that beta2 AR in bilateral VG and AMPK alpha2 in the ipsilateral VG might play important signaling roles after the unilateral labyrinthine damage.

© 2011 Elsevier Ireland Ltd and the Japan Neuroscience Society. All rights reserved.

1. Introduction

Unilateral labyrinthectomy (UL) induces severe postural and oculomotor asymmetry such as barrel rotation, head tilt and spontaneous nystagmus. However, these functional deficits recover gradually after the lesion with no vestibular peripheral regeneration. This phenomenon is referred to as vestibular compensation (Llinas and Walton, 1979; Precht and Dieringer, 1985) and has been used as a model of lesion-induced neuronal plasticity in the central nervous system. It is well known that subjects after the vestibular labyrinthine damage have a much more advantage to get prompt accomplishment of vestibular compensation than those after vestibular ganglion (VG) damage both in basic (Cass and Goshgarian, 1991) and clinical studies (Gacek and Gacek, 1996; Badke et al., 2002; Kitahara et al., 2005a). To date, the molecular events in VG have not been clarified yet.

Recently, it has been revealed that mitochondrial uncoupling proteins (UCPs) in bilateral VG were up-regulated after UL (Kitahara et al., 2007). The changes in molecular expression in VG contralateral to UL side could be one of the important keys to access the mechanisms in vestibular compensation. UCPs are a proton transporter family located in the mitochondrial inner membrane. So far, five molecules have been identified as members of the UCP family. UCP2, UCP4 and brain mitochondrial carrier protein-1 (BMCP-1, i.e. UCP5) were expressed in the central nervous system (Yu et al., 2000) and discussed to have neuro-synaptic and neuro-protective effects (Andrews et al., 2005).

In the present study, to elucidate the molecular events in bilateral VG after UL and understand the role of bilateral VG in vestibular compensation, we examined quantitative changes in mRNA expression of beta-adrenergic receptors (bARs) and AMP-activated protein kinase alpha catalytic subunits (aAMPKs), both of which have been proven to regulate UCPs mRNA expression intracellularly in brown adipose tissue, skeletal muscle, heart, liver and brain (Collins et al., 2001; Jezek, 2002; Andrews et al., 2005; Scharf et al., 2008; Chaudhary and Pfluger, 2009), in bilateral VG after UL.

Abbreviations: aAMPK, AMP-activated protein kinase alpha catalytic subunit; bAR, beta-adrenergic receptor; CT, cycle threshold; LIR, like immunoreactivity; PCR, polymerase chain reaction; RT-PCR, reverse transcription-PCR; UCP, uncoupling protein; UL, unilateral labyrinthectomy; VG, vestibular ganglion.

* Corresponding author at: Department of Otolaryngology, Osaka University, School of Medicine, 2-2 Yamada-oka, Suita-city, Osaka 565-0871, Japan.
Tel.: +81 6 6879 3951; fax: +81 6 6879 3959.
E-mail address: tkitahara@ent.med.osaka-u.ac.jp (T. Kitahara).

0168-0102/$ – see front matter © 2011 Elsevier Ireland Ltd and the Japan Neuroscience Society. All rights reserved.
doi:10.1016/j.neures.2011.11.007

Author's personal copy

2. Materials and methods

Experimental procedures involving animals reported in this study were performed according to animal ethical guidelines and were approved by University of Pittsburgh, School of Medicine.

2.1. Surgical procedure

Male Sprague-Dawley rats weighing 100 g were anesthetized with ether inhalation. The animals received right UL according to the previous paper (Goto et al., 1997; Kitahara et al., 2007). The right bulla was exposed on one side by blunt dissection via a skin incision near the angle of the mandible, and a pediatric otic speculum was placed over the bone to maintain retraction of soft tissues. The ventral surface of the bulla was removed with a fine dental burr and microrongeurs to expose the middle ear cavity. The base of the cochlea was opened with a dental burr and small picks to expose the vestibule and the otolith organs, and semicircular canal cristae were ablated with a curette and aspiration. This procedure ablates the neuroepithelium, without involvement of the ossicular chain, tympanic membrane, internal acoustic canal, cochlear nerve, facial nerve or VG. At the end of surgery, antibiotic cream (Furacin) was topically applied to the opened labyrinth to prevent infection and the temporal bone was sealed with dental cement. The operative wound was sutured and the animal was allowed to recover in light. Histological examination after UL showed that the surgical destruction of the membranous labyrinth had been achieved and that no vestibular hair cells had regenerated as reported previously (Goto et al., 1997; Kitahara et al., 2007). Through this surgical procedure, cochlear organ of Corti was little or roughly damaged but vestibular endo-organ was uniformly destroyed. Therefore, vestibular results were worth while to discuss the role of bARs and aAMPKs in the vestibular system in the present study.

2.2. Tissue preparation

One (1 d, $n=5$), seven (1 w, $n=5$), fourteen (2 w, $n=5$) and twenty-eight days (1 m, $n=5$) after the operation, animals were given a pentobarbital overdose (85 mg/kg, i.p.). Sham controls were also prepared (cont., $n=5$). For real-time PCR studies, the animals were decapitated after cessation of spontaneous respiration and bilateral VG tissues were dissected immediately under a stereomicroscope in chilled phosphate buffered saline (pH 7.2–7.4) and frozen with dry ice powder.

2.3. Total RNA extraction

Total RNA was extracted from each dissected frozen tissue using TRIzol reagents (Gibco BRL). Briefly, each sample was homogenized in 0.8 ml of TRIzol reagent. Chloroform was then added and the mixture was centrifuged in order to separate the RNA phase from the DNA phase. The RNA phase was used for RNA precipitation using isopropyl alcohol. The RNA samples were rinsed with ethanol and dissolved with RNase-free water. Finally, the RNA samples were treated with RNase-free Dnase I (Roche) to remove contaminated genomic DNAs before reverse transcription.

2.4. Reverse transcription of RNA

The reverse transcription mixture included 10 μl of 10× PCR Taq Gold buffer II (Applied Biosystems), 30 μl of 25 mM $MgCl_2$, 4 μl of 25 mM of each dNTP, 5 μl of 100 μM of random primers (Gibco BRL), 2 μl of RNasin (40 units; Applied Biosystems), 1.25 μl of Super-Script II (250 units; Applied Biosystems) and 5 μl (250 ng) of DNA-free total RNA in a final volume of 100 μl. The mixture was incubated at 25 °C for 10 min, 48 °C for 30 min and 95 °C for 5 min in a 9600 Thermocycler (Applied Biosystems).

Table 1
Gene-specific primers for PCR of rat beta-adrenergic receptors, AMP-activated protein kinase alpha subunits and 18S rRNA.

Beta1AR (accession no. NM_012701)
Forward primer 5′-TCGCGCCTCGTGGCTCTGCG-3′
Reverse primer 5′-GAAGGAGCCCCGGGGACGG-3′
Beta2AR (accession no. NM_012492)
Forward primer 5′-GTTGTGCGTCACAGCCAGCA-3′
Reverse primer 5′-AGATACGATAGAGGAAGCGA-3′
Beta3AR (accession no. NM_013108)
Forward primer 5′-AGTGGGACTCCTCGTAATG-3′
Reverse primer 5′-CGCTTAGCTACGACGAAC-3′
AMPKa1 (accession no. NM_001013367)
Forward primer 5′-GACGGCCGAGAAGCAGAAGC-3′
Reverse primer 5′-TACAGATATAATCAAATAGC-3′
AMPKa2 (accession no. NM_178143)
Forward primer 5′-AAGCAGAAGCACGACGGGCG-3′
Reverse primer 5′-GGAAGAGCCGGCGCGCAACC-3′
18SrRNA (accession no. X00686)
Forward primer 5′-TCCGACCATAAACGATGCCGACT-3′
Reverse primer 5′-TCCTGGTGGTGCCCTTCCGTCAAT-3′

AR, adrenergic receptor; AMPK, AMP-activated protein kinase.

2.5. Reverse-transcriptase PCR

This study examined mRNA expression patterns of five kinds of molecules, i.e. beta1,2,3 ARs and AMPK alpha1,2 subunits, in VG and spiral ganglion (SG). The endogenous PCR primers specific to target molecules were designed using Primer Express software (Perkin Elmer) as shown in Table 1. Samples with reverse transcriptase were forwarded for PCR (95 °C for 12 min and, 35 cycles at 95 °C for 15 s and 60 °C for 1 min) and electrophoresed on 1.5% agarose gel to check the results of reverse-transcriptase PCR. Samples without reverse transcription were also forwarded for PCR as negative controls to make sure of no genomic DNA contamination.

PCR products were electrophoresed on 3% Seakem GTG agarose gel (FMC Bioproducts) and purified using QIA quick Gel Extraction Kit (QIAGEN). Sequencing was accomplished by means of ABI Prism dRhodamine Terminator Cycle Sequencing Ready Reaction Kit with ABI 310 DNA sequencer (Applied Biosystems).

2.6. Real-time quantitative PCR

Quantitative comparisons of mRNA expression profiles of four kinds of molecules, i.e. beta1,2 ARs and AMPK alpha1,2 subunits, in VG were examined by means of real-time quantitative PCR. PCR reactions were performed in the presence of the oligonucleotide primers for beta1,2 ARs, AMPK alpha1,2 subunits and 18S rRNA shown in Table 1 and quantified by SYBR Green PCR reagents (Applied Biosystems). Rat 18S rRNA, an endogenous housekeeping gene, was used as an internal control for this method. Each sample determination was performed in triplicate.

The PCR mixture included 5 μl of 10× SYBR PCR buffer, 6 μl of 25 mM $MgCl_2$, 4 μl of each dNTP (blended with 2.5 mM dATP, dGTP and dCTP, and 5 mM dUTP), 2.5 μl of each gene-specific primer (5 μM), 0.5 μl of AmpErase UNG (0.5 units), 0.25 μl of AmpliTaq Gold (1.25 units) and 5 μl of cDNA (250 ng) in a final volume of 50 μl. The conditions for the real-time PCR were as follows: 50 °C for 2 min, 95 °C for 12 min and, 35 cycles at 95 °C for 15 s and 60 °C for 1 min in ABI PRISM 7700 Sequence Detection System (Applied Biosystems). 7700 Sequence Detection software was used for instrument control, automated data collection and data analysis.

Author's personal copy

2.7. Data analysis

The number of PCR cycles was recorded until the fluorescence intensity exceeded the pre-determined threshold. The quantification of the initial amounts of template molecules relied on this number of PCR cycles, which is termed the cycle threshold (CT). The dCT represents the CT of the target gene normalized to the rat endogenous 18S rRNA ($dCT = CT_{target} - CT_{18SrRNA}$). Relative quantification of the mRNA expression levels of target genes (=fold range) was calculated using the 2^{-ddCT} method, where $ddCT = (CT_{target} - CT_{18SrRNA})_A - (CT_{target} - CT_{18SrRNA})_B$ (Schmittgen et al., 2000). For example, changes in the gene expression of each target bAR (bARn) in VG after UL ($TIME_x$) were quantified as the fold range: 2^{-ddCT} ($ddCT = (CT_{bARn} - CT_{18SrRNA})_{TIME_x} - (CT_{bARn} - CT_{18SrRNA})_{CONTROL}$). Changes in the gene expression of each target aAMPK (aAMPKn) in VG after UL ($TIME_x$) were quantified as the fold range: 2^{-ddCT} ($ddCT = (CT_{aAMPKn} - CT_{18SrRNA})_{TIME_x} - (CT_{aAMPKn} - CT_{18SrRNA})_{CONTROL}$).

Differences in expression of each target molecule among three groups were examined by Fisher's PLSD-test. p values under 0.05 were considered as significant.

2.8. Immunohistochemistry

The animals were euthanized with sodium pentobarbital (85 mg/kg, i.p.) and perfused transcardially with 0.1 M PBS, followed by paraformaldehyde–lysine–periodate fixative. Temporal bones were post-fixed in 4% paraformaldehyde for 24 h at room temperature, decalcified in 10% formic acid to chemical testing criterion, neutralized in overnight 5% sodium sulfate and infiltrated with OCT compound as described previously (Goto et al., 1997; Kitahara et al., 2007).

The 5 μm thick sections cryostat sections were incubated sequentially in the following solutions at RT: 0.1% TritonX-100 and 2% bovine serum albumin (BSA) in 0.1 M PBS for 2 h; antisera against Beta2 AR (cat#ab36956) and AMPK alpha2 anti-rabbit polyclonal antiboies (cat#ab3760) (Abcam Corporation; diluted 1:1000) in the same solution for 48 h; 0.1 M PBS for 15 min; biotinylated goat anti-rabbit IgG (Vector Laboratories; diluted 1:250) in 2% BSA in 0.1 M PBS for 24 h; 0.1 M PBS for 15 min; Vectastain ABC reagent (Vector Laboratories; diluted 1:100) for 1 h; 0.1 M PBS for 15 min; 5 mg/ml diaminobenzidine tetrahydrochloride (DAB)/0.01% H_2O_2 in 0.05 M Tris buffer for 5 min, and then examined under a light microscope. For negative controls, primary antibodies were either preabsorbed with each control peptide (1:50) or the primary antibody was omitted.

3. Results

Simple PCR products as a pilot study revealed that beta1,2 ARs and AMPK alpha1,2 subunits in VG and SG were detected on the gel at the expected size (Fig. 1) as reported previously (Fauser et al., 2004; Khan et al., 2007). Using the 2^{-ddCT} method as bAR and aAMPK mRNA expression in the VG contralateral to the sham operated side in 1 (beta1 AR: 1.04 ± 0.25; beta2 AR: 1.01 ± 0.19; AMPK alpha1: 0.095 ± 0.40; AMPK alpha2: 1.02 ± 0.22) (Schmittgen et al., 2000), no significant change in mRNA expressions of these molecules was observed in the VG ipsilateral to the sham operated side (beta1 AR: 1.22 ± 0.38; beta2 AR: 1.05 ± 0.30; AMPK alpha1: 1.12 ± 0.45; AMPK alpha2: 1.25 ± 0.44).

In the ipsilateral VG (Fig. 2; re: bAR and aAMPK expression in the ipsilateral VG = 1 in sham 0 d), mRNA expressions of beta2 AR mRNA among bARs and AMPK alpha2 mRNA among aAMPKs were significantly up-regulated with the maximum increase at the postoperative 7 d (beta2 AR: 3.20 ± 0.35 (*$p < 0.05$)) and 1 d

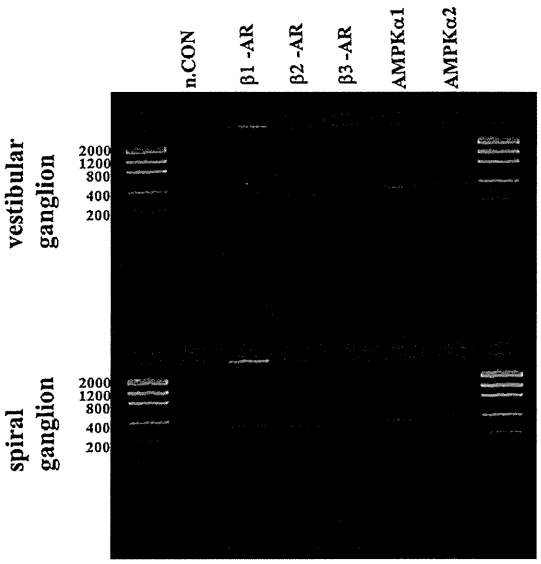

Fig. 1. Expression of mRNAs of beta adrenergic receptor and AMP-activated protein kinase alpha subunit mRNAs in the inner ear. Amplified cDNAs of beta-1,2 adrenergic receptors (ARs) and AMP-activated protein kinase (AMPK) alpha-1,2 subunits of expected size were observed clearly in vestibular ganglion (VG). Samples without reverse transcription were forwarded for PCR as negative controls (n.CON) to ascertain that there was no genomic DNA contamination.

(AMPK alpha2: 4.84 ± 0.34 (*$p < 0.05$)), respectively. AMPK alpha2 mRNA returned to the control level 7 d after UL (AMPK alpha2: 1.41 ± 0.48 ($p > 0.05$)). Beta2 AR mRNA expression was significantly up-regulated even 28 d after UL (beta2 AR: 2.00 ± 0.36 (*$p < 0.05$)).

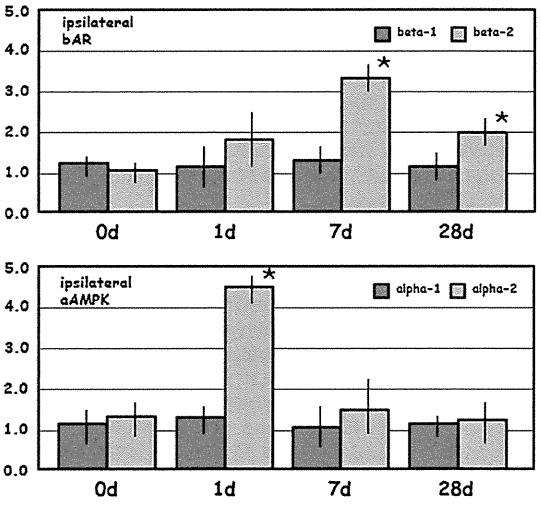

Fig. 2. Changes in mRNAs of beta-adrenoreceptor and AMP activated protein kinase-alpha in the ipsilateral vestibular ganglion after labyrinthectomy. In the ipsilateral vestibular ganglion (VG) (re: beta-adrenergic receptor (bAR) and AMP-activated protein kinase alpha subunit (aAMPK) expressions in the ipsilateral VG = 1 in sham 0 d), mRNA expressions of beta2 AR mRNA among bARs and AMPK alpha2 mRNA among aAMPKs were significantly up-regulated with the maximum increase at the postoperative 7 d (beta2 AR: 3.20 ± 0.35 (*$p < 0.05$)) and 1 d (AMPK alpha2: 4.84 ± 0.34 (*$p < 0.05$)), respectively. AMPK alpha2 mRNA returned to the control level at the postoperative 7 d (AMPK alpha2: 1.41 ± 0.48 ($p > 0.05$)). Beta2 AR mRNA expression was significantly up-regulated even at the postoperative 28 d (beta2 AR: 2.00 ± 0.36 (*$p < 0.05$)).

Author's personal copy

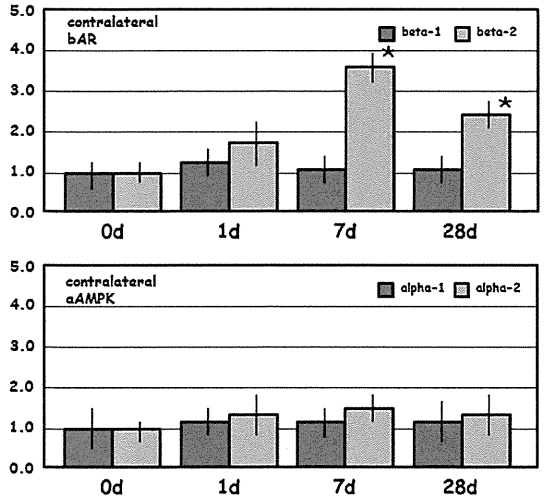

Fig. 3. Changes in mRNAs of beta-adrenoreceptor and AMP activated protein kinase-alpha in the contralateral vestibular ganglion after labyrinthectomy. In the contralateral vestibular ganglion (VG) (re: beta-adrenergic receptor (bAR) and AMP-activated protein kinase alpha subunit (aAMPK) expressions in the contralateral VG = 1 in sham 0 d), only beta2 AR mRNA expression was gradually up-regulated between 7 d (beta2 AR: 3.35 ± 0.46 ($^*p < 0.05$)) and 28 d (beta2 AR: 2.23 ± 0.39 ($^*p < 0.05$)) after surgery.

In the contralateral VG (Fig. 3; re: bAR and aAMPK expression in the contralateral VG = 1 in sham 0 d), only beta2 AR mRNA expression was gradually up-regulated between 7 d (beta2 AR: 3.35 ± 0.46 ($^*p < 0.05$)) and 28 d (beta2 AR: 2.23 ± 0.39 ($^*p < 0.05$)) after UL.

In decalcified, cryostat sectioned temporal bones, both beta2 AR-LIR (Fig. 4A) and AMPK alpha2-LIR (Fig. 5A) were observed in the form of punctuate deposits and distributed uniformly within the cytoplasm of VG cells. Beta2 AR-LIRs were increased in bilateral VG 7 d (Fig. 4B and C) and still 28 d after UL (Fig. 4D), whereas AMPK alpha2-LIRs were up-regulated in the ipsilateral VG 1 d (Fig. 5B), not 7 d after UL (Fig. 5C) or in the contralateral side (Fig. 5D). Negative controls in both immunohistochemical studies were confirmed but data not shown.

4. Discussion

AMPKs are located in the mitochondrial membrane and composed of catalytic and regulatory subunits (Sanz, 2008). They are activated according to the intracellular ATP/AMP ratio, which is elevated in response to the oxidative stress. The activated kinases can transcript mRNA of UCP family members in various kinds of tissues (Scharf et al., 2008; Chaudhary and Pfluger, 2009). In the previous studies, responses of UCPs 1–3 to superoxide application were an antioxidant protective mechanism (Echtay et al., 2002). Up-regulation of UCPs 2–4 was observed in the mouse inner ear ganglia after aminoglycoside intoxication and blocked by co-administration of the antioxidant (Kitahara et al., 2005b). At that time, aAMPKs were revealed to behave in the same manner as UCPs did (unpublished data). In the present study, up-regulation of AMPK alpha2 was seen in the ipsilateral VG transiently after UL as that of UCPs 2–4 was (Kitahara et al., 2007). All taken together, the mitochondrial AMPK-UCP signaling could play a neuro-protective role against oxidative damage in the eighth nerve. Actually, UL did acute damages to the ipsilateral epithelia-neuronal synapses (Kitahara et al., 2007). Therefore, rapid responses of AMPK alpha2 and UCPs 2–4 in the eighth nerve could make a neuro-protective

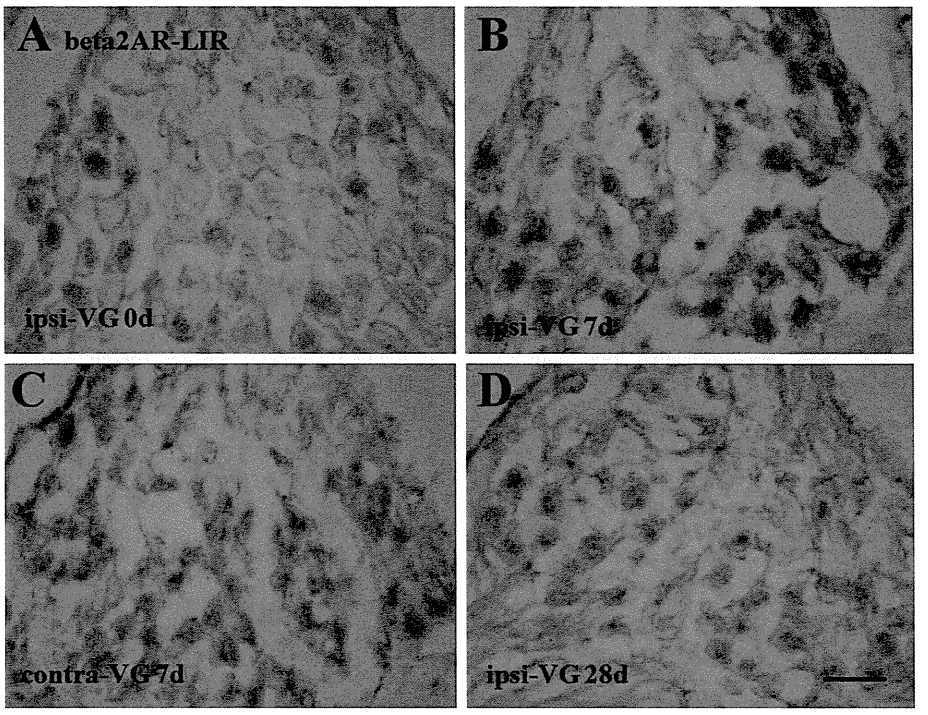

Fig. 4. Beta2 adrenergic receptor-like immunoreactivity in the vestibular ganglion cells. (A) Beta2 adrenergic receptor (AR)-like immunoreactivity (LIR) formed punctate deposits uniformly distributed around the cell somata of vestibular ganglion (VG) in control animals. (B and C) Beta2 AR-LIRs were increased in bilateral VG 7 d and (D) still 28 d after unilateral labyrinthectomy. Bar = 50 μm.

Author's personal copy

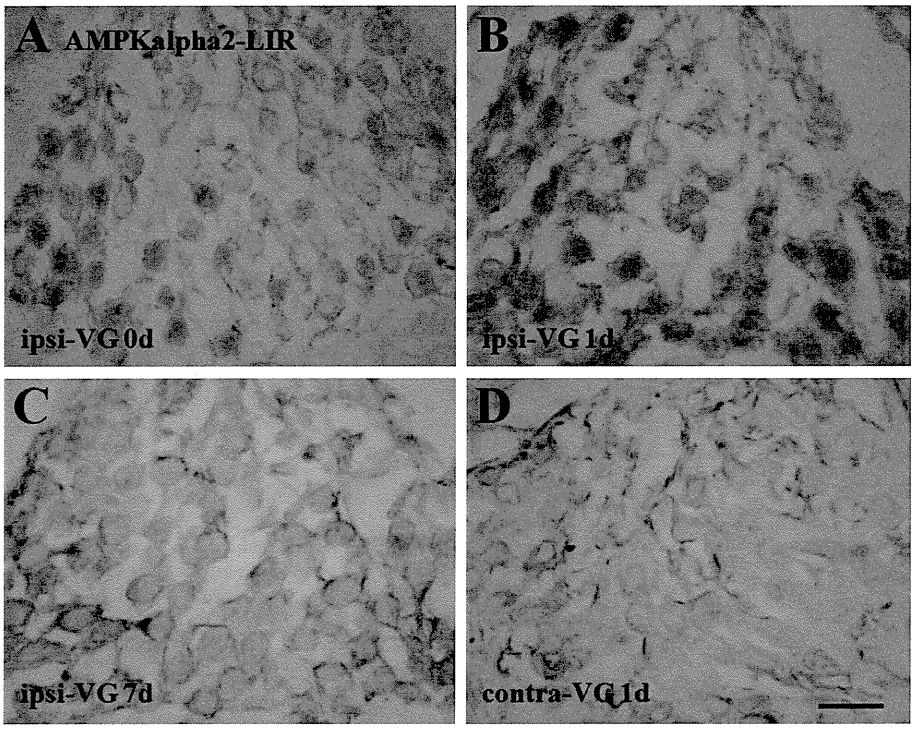

Fig. 5. AMP-activated protein kinase alpha2 subunit-like immunoreactivity in the vestibular ganglion cells. (A) AMP-activated protein kinase (AMPK) alpha2 subunit-like immunoreactivity (LIR) formed punctate deposits uniformly distributed around the cell somata of vestibular ganglion (VG) in control animals. (B) AMPK alpha2-LIRs were increased in the ipsilateral VG 1 d, (C) not 7 d after unilateral labyrinthectomy or (D) in the contralateral side. Bar = 50 μm.

role against oxidative damage in the ipsilateral epithelia-neuronal synapses after UL.

AR subunits are located in the inner ear and alpha1,2 in the artery (Laurikainen et al., 1994; Gruber et al., 1998), beta1 in the stria vascularis (Wangemann et al., 2000; Fauser et al., 2004) and dark cells (Wangemann et al., 1999; Fauser et al., 2004), and beta2 in the endolymphatic sac (Mori and Uozumi, 1991; Inamoto et al., 2009). Previous papers suggest that ARs have regulatory effects of vaso-diameter (Laurikainen et al., 1994; Gruber et al., 1998) and endolymphatic fluid homeostasis (Mori and Uozumi, 1991; Wangemann et al., 1999, 2000; Inamoto et al., 2009), however the role of ARs in VG has not been clarified yet. They are supposed to be activated by adrenergic innervation from the ipsilateral supra cervical ganglion (Hozawa and Kimura, 1989; Yamashita et al., 1992; Gil-Loyzaga et al., 1998). Beta-adrenergic inputs can transcript mRNA of UCP family members in various kinds of tissues (Collins et al., 2001; Jezek, 2002). In the previous studies, UCP2 and 3 as well as UCP1 were thermogenic in yeast (Paulik et al., 1998; Hinz et al., 1999) and brain UCP2 was suggested to modulate pre- and post-synaptic events by axonal thermogenesis (Andrews et al., 2005). In the present study, delayed up-regulation of beta2 AR was seen in bilateral VG and long lasting after UL as that of UCP2 was (Kitahara et al., 2007). All taken together, the mitochondrial AR-UCP signaling could play a thermal signaling role for neuro-modulation in the eighth nerve. Since UL did not do any direct damages to the contralateral side, the delayed up-regulation of beta2 AR in bilateral VG might play an important role in long-term maintenance for central vestibular synapses, possibly regarded with vestibular compensation. According to our previous papers (Kitahara et al., 1995, 1997), vestibular rebalancing neuronal circuits by way of vestibular commissures and/or cerebellum were turned on immediately after UL and turned off around 2–4 weeks after the lesion. Therefore, the delayed up-regulation of beta2 AR mRNA in bilateral VG could regulate the neuronal circuits by way of vestibular commissures and/or cerebellum after UL. Since supra cervical ganglionectomy (Bielefeld and Henderson, 2007) or dopamine beta hydroxylase knockout study (Maison et al., 2010) could not have any significant influences on noise-induced inner ear damages, AR-UCP signaling could not be related with neuro-protection but mainly with neuro-modulation in the eighth nerve.

According to the previous literatures (Sanz, 2008; Quentin et al., 2011), it is still hard to explain the specific physiological significance of beta2 AR and AMPK alpha2 among all the bARs and aAMPKs in vestibular compensation for now. Among bARs, only beta1 and beta2 exist in the inner ear. Among bARs, only beta2 and beta3 are possible UCP mRNA transcript regulators in various kinds of tissues including the nervous system. Therefore, beta2 AR might be predominantly up-regulated among bARs through adrenergic inputs after UL to regulate beta2-related mRNA transcripts like UCP in the inner ear. As to aAMPKs, there have been no suggestive reports in subunit details in various kinds of tissues including the nervous system. Further experiments of each subunit in the inner ear should be reported in later communications.

The mechanisms of the delayed up-regulation of beta2 AR mRNA in the contralateral VG after UL are quite interesting. One of the possible mechanisms might be supra cervical ganglion-mediated (Hozawa and Kimura, 1989; Yamashita et al., 1992; Gil-Loyzaga et al., 1998). Supra cervical ganglion includes abundant catecholamines and activates catecholaminergic receptors by transcapillary diffusion into vestibular neurons and/or epithelia rather than direct contact with them. In our preliminary experiments, kanamycin oto-toxicity and bilateral labyrinthectomies both could do damage to bilateral inner ears simultaneously but induce no significant change in beta2 AR expression in vestibular

Author's personal copy

peripheries (unpublished data). Therefore, the great imbalance between bilateral vestibular nuclei activities and subsequent activation of superior cervical ganglion after unilateral vestibular ablation might be essential for adrenergic inputs into bilateral VG, resulting in long-lasting beta2 AR up-regulation in the bilateral VG for vestibular neuro-modulation in the bilateral sides.

Another important purpose of this paper was to understand the status of VG during vestibular compensation. In the previous clinical literatures, as compared dizzy patients after labyrinthectomy with those after vestibular neurectomy, the former patients were less annoyed by postoperative motion-evoked dizziness than the latter ones (Gacek and Gacek, 1996; Badke et al., 2002). In the previous basic literatures, labyrinthectomized animals showed more rapid recovery from vestibulo-occular reflex asymmetries than vestibular ganglionectomized ones (Cass and Goshgarian, 1991). All these findings with the present study suggest that long-lasting bilateral VG responses possibly mediated by beta2 AR could contribute to the successful accomplishment of central vestibular neuro-plasticity after acute vestibular peripheral damage. Further studies are needed to elucidate molecular mechanisms of bilateral VG-mediated vestibular compensation.

Conflict of interest

None.

Acknowledgements

We thank Professor Carey D. Balaban (Department of Otolaryngology, University of Pittsburgh, School of Medicine) for helpful advice and support. We also thank Dr. Yasusuke Yamagiwa, a registered statistician (certificate number: 0540072), for helpful advice of statistical analysis. This study was supported in part by a Health Science Research Grant for Specific Disease from the Ministry of Health, Labour and Welfare, Japan (2011–2013).

References

Andrews, Z.B., Diano, S., Horvath, T.L., 2005. Mitochondrial uncoupling proteins in the CNS: in support of function and survival. Nat. Rev. Neurosci. 6, 829–840.
Badke, M.B., Pyle, G.M., Shea, T., et al., 2002. Outcomes in vestibular ablative procedures. Otol. Neurotol. 23, 504–509.
Bielefeld, E.C., Henderson, D., 2007. Influence of sympathetic fibers on noise-induced hearing loss in the chinchilla. Hear. Res. 223, 11–19.
Cass, S.P., Goshgarian, H.G., 1991. Vestibular compensation after labyrinthectomy and vestibular neurectomy in cats. Otolaryngol. Head Neck Surg. 104, 14–19.
Chaudhary, N., Pfluger, P.T., 2009. Metabolic benefits from Sirt1 and Sirt1 activators. Curr. Opin. Clin. Nutr. Metab. Care 12, 431–437.
Collins, S., Cao, W., Daniel, K.W., Dixon, T.M., Medvedev, A.V., Onuma, H., Surwit, R., 2001. Adrenoceptors, uncoupling proteins, and energy expenditure. Exp. Biol. Med. 226, 982–990.
Echtay, K.S., Roussel, D., St-Pierre, J., Jekabsons, M.B., Cadenas, S., Stuart, J.A., Harper, J.A., Roebuck, S.J., Morrison, A., Pickering, S., Clapham, J.C., Brand, M.D., 2002. Superoxide activates mitochondrial uncoupling proteins. Nature 415, 96–99.
Fauser, C., Schimanski, S., Wangemann, P., 2004. Localization of beta1-adrenergic receptors in the cochlea and the vestibular labyrinth. J. Membr. Biol. 201, 25–32.
Gacek, R.R., Gacek, M.R., 1996. Comparison of labyrinthectomy and vestibular neurectomy in the control of vertigo. Laryngoscope 106, 225–230.
Gil-Loyzaga, P., Vicente-Torres, M.A., Arce, A., Cardinali, D.P., Esquifino, A., 1998. Effect of superior cervical ganglionectomy on catecholamine concentration in rat cochlea. Brain Res. 779, 53–57.
Goto, M.M., Romero, G.G., Balaban, C.D., 1997. Transient changes in flocculonodular lobe protein kinase C expression during vestibular compensation. J. Neurosci. 17, 4367–4381.
Gruber, D.D., Dang, H., Shimozono, H., Scofield, M.A., 1998. Wangemann P: alpha 1A-adrenergic receptors mediate vasoconstriction of the isolated spiral modiolar artery in vitro. Hear. Res. 119, 113–124.
Hinz, W., Faller, B., Grüninger, S., Gazzotti, P., Chiesi, M., 1999. Recombinant human uncoupling protein-3 increases thermogenesis in yeast cells. FEBS Lett. 448, 57–61.
Hozawa, K., Kimura, R.S., 1989. Vestibular sympathetic nervous system in guinea pig. Acta Otolaryngol. 107, 171–181.
Inamoto, R., Miyashita, T., Akiyama, K., Mori, T., Mori, N., 2009. Endolymphatic sac is involved in the regulation of hydrostatic pressure of cochlear endolymph. Am. J. Physiol. Regul. Integr. Comp. Physiol. 297, 1610–1614.
Jezek, P., 2002. Possible physiological roles of mitochondrial uncoupling proteins – UCPn. Int. J. Biochem. Cell Biol. 34, 1190–1206.
Khan, K.M., Drescher, M.J., Hatfield, J.S., Ramakrishnan, N.A., Drescher, D.G., 2007. Immunohistochemical localization of adrenergic receptors in the rat organ of corti and spiral ganglion. J. Neurosci. Res. 85, 3000–3012.
Kitahara, T., Takeda, N., Saika, T., Kubo, T., Kiyama, H., 1995. Effects of MK801 on Fos expression in the rat brainstem after unilateral labyrinthectomy. Brain Res. 700, 182–190.
Kitahara, T., Takeda, N., Saika, T., Kubo, T., Kiyama, H., 1997. Role of the flocculus in the development of vestibular compensation: immunohistochemical studies with retrograde tracing and flocculectomy using Fos expression as a marker in the rat brainstem. Neuroscience 76, 571–580.
Kitahara, T., Takeda, N., Nishiike, S., Okumura, S., Kubo, T., 2005a. Prognosis of inner ear periphery and central vestibular plasticity in sudden deafness with vertigo. Ann. Otol. Rhinol. Laryngol. 114, 786–791.
Kitahara, T., Li, H.S., Balaban, C.D., 2005b. Regulation of mitochondrial uncoupling proteins in mouse inner ear ganglion cells in response to systemic kanamycin challenge. Neuroscience 135, 639–653.
Kitahara, T., Horii, A., Kizawa, K., Maekawa, C., Kubo, T., 2007. Changes in mitochondrial uncoupling protein expression in the rat vestibular nerve after labyrinthectomy. Neurosci. Res. 59, 237–242.
Laurikainen, E.A., Costa, O., Miller, J.M., Nuttall, A.L., Ren, T.Y., Masta, R., Quirk, W.S., Robinson, P.J., 1994. Neuronal regulation of cochlear blood flow in the guinea-pig. J. Physiol. 480, 563–573.
Llinas, R., Walton, K., 1979. Vestibular compensation: a distributed property of the central nervous system. In: Asanuma, H., Wilson, V.J. (Eds.), Integration in the Nervous System. Igaku Shoin, Tokyo, pp. 145–166.
Maison, S.F., Le, M., Larsen, E., Lee, S.K., Rosowski, J.J., Thomas, S.A., Liberman, M.C., 2010. Mice lacking adrenergic signaling have normal cochlear responses and normal resistance to acoustic injury but enhanced susceptibility to middle-ear infection. J. Assoc. Res. Otolaryngol. 11, 449–461.
Mori, N., Uozumi, N., 1991. Evidence that beta 2-receptors mediate action of catecholamines on endolymphatic sac DC potential. Am. J. Physiol. 260, 911–915.
Paulik, M.A., Buckholz, R.G., Lancaster, M.E., Dallas, W.S., Hull-Ryde, E.A., Weiel, J.E., Lenhard, J.M., 1998. Development of infrared imaging to measure thermogenesis in cell culture: thermogenic effects of uncoupling protein-2, troglitazone and β-adrenoceptor agonists. Pharm. Res. 15, 944–949.
Precht, W., Dieringer, N., 1985. Neuronal events paralleling functional recovery (compensation) following peripheral vestibular lesions. In: Berthoz, A., Melvill Jones, G. (Eds.), Adaptive Mechanism in Gaze Control, Facts and Theories. Elsevier, Amsterdam, pp. 251–268.
Quentin, T., Kitz, J., Steinmetz, M., Poppe, A., Bär, K., Krätzner, R., 2011. Different expression of the catalytic alpha subunits of the AMP activated protein kinase – an immunohistochemical study in human tissue. Histol. Histopathol. 26, 589–596.
Sanz, P., 2008. AMP-activated protein kinase: structure and regulation. Curr. Protein Pept. Sci. 9, 478–492.
Scharf, M.T., Naidoo, N., Zimmerman, J.E., Pack, A.I., 2008. The energy hypothesis of sleep revisited. Prog. Neurobiol. 86, 264–280.
Schmittgen, T.D., Zakrajsek, B.A., Mills, A.G., Gorn, V., Singer, M.J., Reed, M.W., 2000. Quantitative reverse transcription polymerase chain reaction to study mRNA decay: comparison of endpoint and real-time methods. Anal. Biochem. 285, 194–204.
Wangemann, P., Liu, J., Shimozono, M., Scofield, M.A., 1999. Beta1-adrenergic receptors but not beta2-adrenergic or vasopressin receptors regulate K+ secretion in vestibular dark cells of the inner ear. J. Membr. Biol. 170, 67–77.
Wangemann, P., Liu, J., Shimozono, M., Schimanski, S., Scofield, M.A., 2000. K+ secretion in strial marginal cells is stimulated via beta 1-adrenergic receptors but not via beta 2-adrenergic or vasopressin receptors. J. Membr. Biol. 175, 191–202.
Yamashita, H., Bagger-Sjoback, D., Sekitani, T., 1992. Distribution of tyrosine hydroxylase-like immunofluorescence in guinea pig vestibular ganglia and sensory areas. Auris Nasus Larynx 19, 63–68.
Yu, X.X., Mao, W., Zhong, A., Schow, P., Brush, J., Sherwood, S.W., Adams, S.H., Pan, G., 2000. Characterization of novel UCP5/BMCP1 isoforms and differential regulation of UCP4 and UCP5 expression through dietary or temperature manipulation. FASEB J. 14, 1611–1618.

Acta Oto-Laryngologica, 2013; 133: 373–377

informa
healthcare

ORIGINAL ARTICLE

Vestibular and cochlear neuritis in patients with Ramsay Hunt syndrome: a Gd-enhanced MRI study

HIDETAKA IWASAKI[1], NAOKI TODA[1], MIKA TAKAHASHI[1], TAKAHIRO AZUMA[1], KATSUHIKO NAKAMURA[1], SHO-ICHIRO TAKAO[2], MASAFUMI HARADA[2] & NORIAKI TAKEDA[1]

[1]*Department of Otolaryngology and* [2]*Department of Radiology, Institute of Health Biosciences, University of Tokushima Graduate School, Tokushima, Japan*

Acta Otolaryngol Downloaded from informahealthcare.com by (D)Tokushima U Kuramoto on 02/04/14
For personal use only.

Abstract

Conclusion: It is suggested that vertigo in patients with Ramsay Hunt syndrome is mostly induced by superior vestibular neuritis consecutive to the reactivation of varicella-zoster virus (VZV) infection from the geniculate ganglion through the faciovestibular anastomosis. Refractory hearing loss in patients with Ramsay Hunt syndrome may be due to cochlear neuritis following the spread of VZV. *Objectives:* An attempt was made to selectively identify vestibulocochlear nerves in the internal auditory canal (IAC) on gadolinium (Gd)-enhanced MRI in patients with Ramsay Hunt syndrome. *Methods:* Fourteen patients with Ramsay Hunt syndrome presenting with facial palsy, herpes zoster oticus, vertigo, and/or sensorineural hearing loss were scanned on 1.5 T MRI enhanced with Gd. Perpendicular section images of the IAC were reconstructed to identify the facial, superior, and inferior vestibular nerves and the cochlear nerves separately. *Results:* All except one of the patients with Ramsay Hunt syndrome with vertigo showed both canal paresis on the caloric test and Gd enhancement of the superior vestibular nerve in the IAC on MRI. Among 10 patients with hearing loss, 3 patients with severe to moderate sensorineural hearing loss showed Gd enhancement of the cochlear nerve in the IAC on MRI.

Keywords: *Facial palsy, varicella zoster virus, vestibular nerves, vestibulocochlear nerves*

Introduction

Ramsay Hunt syndrome is characterized by herpes zoster oticus, peripheral facial palsy, and eighth cranial nerve symptoms including vertigo and hearing loss [1]. Ramsay Hunt syndrome is caused by the reactivation of varicella-zoster virus (VZV) infected latently in the geniculate ganglion of the seventh cranial nerve. Reactivated VZV in the geniculate ganglion induces the inflammation of the facial nerve, resulting in facial palsy [2]. Since gadolinium-DTPA (Gd) accumulates in the inflamed tissue where there is a breakdown of the blood–nerve barrier, Gd-enhanced magnetic resonance imaging (MRI) can visualize the inflammation of the cranial nerves. Therefore, Gd-enhanced MRI studies have reported a high frequency of enhancement in the regions of the internal auditory canal (IAC) and/or the intratemporal segments of the facial nerve in patients with Ramsay Hunt syndrome [3].

Because the vestibulocochlear nerves are in proximity to the geniculate ganglion, they are also inflamed by transneural infection from reactivated VZV, leading to the vestibulocochlear symptoms in patients with Ramsay Hunt syndrome [4]. However, the enhancement of the eighth cranial nerves independent from the facial nerve was seldom reported in Gd-enhanced MRI studies in patients with Ramsay Hunt syndrome.

In the present study, an attempt was made to investigate the enhancement of the vestibulocochlear nerves in the IAC on Gd-enhanced MRI in patients

Correspondence: Noriaki Takeda MD PhD, Department of Otolaryngology, Institute of Health Biosciences, University of Tokushima Graduate School, 3-18-15 Kuramoto, Tokushima, 770-8503, Japan. Tel: +81 88 633 7169. Fax: +81 88 633 7170. E-mail: takeda@clin.med.tokushima-u.ac.jp

(Received 5 September 2012; revised 8 November 2012; accepted 11 November 2012)

ISSN 0001-6489 print/ISSN 1651-2251 online © 2013 Informa Healthcare
DOI: 10.3109/00016489.2012.750735

RIGHTSLINK

Table I. Details of the patients in the study (n = 14).

Case no.	Sex	Age (years)	Affected side	HB grade	ENoG	Vertigo	CP	Hearing loss (dB)	FN	SVN	IVN	CN
1	F	72	Left	VI	100%	+	+	88	+	+	+	+
2	F	59	Left	VI	24%	+	+	37	+	+	–	+
3	M	66	Right	VI	100%	+	+	33	+	+	–	+
4	F	45	Right	VI	82%	+	+	23	+	+	–	–
5	M	62	Left	V	52%	+	+	28	–	+	–	–
6	M	41	Left	V	22%	+	+	27	–	+	–	–
7	M	43	Right	VI	100%	+	+	23	–	+	–	–
8	F	60	Left	IV	56%	+	+	20	–	+	–	–
9	F	78	Right	VI	75%	+	+	–	–	+	–	–
10	M	77	Right	V	83%	+	+	–	–	+	–	–
11	M	72	Right	VI	83%	+	+	–	–	+	–	–
12	F	83	Right	V	75%	+	+	–	–	–	–	–
13	M	58	Right	VI	100%	–	–	52	–	–	–	–
14	M	61	Right	IV	21%	–	–	28	–	–	–	–

CN, cochlear nerve; CP, canal paresis on the caloric test; ENoG, electroneurography; FN, facial nerve; HB grade, House-Brackmann grading; Hearing loss, the averaged right–left differences in hearing levels at 2000, 4000, and 8000 Hz; IVN, inferior vestibular nerve; SVN, superior vestibular nerve; +, positive enhancement of Gd-MRI; –, negative enhancement of Gd-MRI.

Acta Otolaryngol Downloaded from informahealthcare.com by (D)Tokushima U Kuramoto on 02/04/14
For personal use only.

with Ramsay Hunt syndrome. For this purpose, MRI images perpendicular to the IAC were reconstructed to identify the facial, superior, and inferior vestibular nerves and the cochlear nerves separately. Correlations between their enhancement and canal paresis (CP) on the caloric test and/or sensorineural hearing loss on pure tone audiometry were also examined.

Material and methods

Fourteen patients with Ramsay Hunt syndrome who showed peripheral facial palsy, ipsilateral herpes zoster oticus, and vertigo/hearing loss (eight males and six females; 41–83 years old; mean age 62.6 years) participated in the present study (Table I). Seven cases had the simultaneous development of facial palsy and vertigo and/or hearing loss, six cases had vertigo and/or hearing loss preceding the development of facial palsy, and one case had facial palsy preceding the development of vertigo and hearing loss. The House-Brackmann (HB) grading of their initial facial palsy ranged from IV to VI. The electroneurography (ENoG) findings ranged from 21% to 100% at 10–14 days after the onset. Twelve and 10 patients complained of vertigo and hearing loss, respectively. Eight patients had both vertigo and hearing loss. Twelve dizzy patients all showed CP on the caloric test performed 16.9 ± 10.6 days after the onset. On the basis of the initial pure tone audiograms, 10 patients showed sensorineural hearing loss. We evaluated the right–left differences in hearing level, because hearing impairment from other causes such as aging and noise exposure were excluded (Figure 1). Within a week after the onset, patients were treated with systemic steroids (methylprednisolone: 250 mg for 3 days, 125 mg for 3 days, 80 mg for 3 days, i.v.) and antiviral agents (valaciclovir: 3000 mg for 7 days, p.o.).

ENoG was performed with the recording surface electrodes on the nasolabial fold. Bipolar rectangular pulses of 0.2 ms duration with stepwise increase of the stimulating current from 35 mA to 50 mA were given by a bipolar stimulator placed on the skin over the stylomastoid foramen, and the maximal compound action potentials were recorded. ENoG value was calculated using the following formula: ENoG

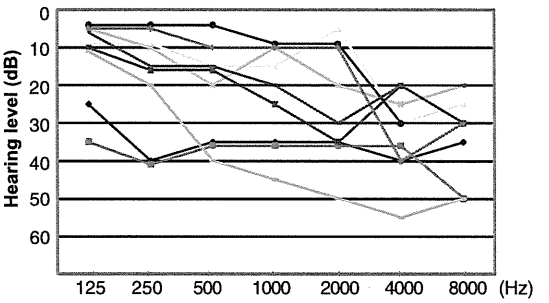

Figure 1. Differences in hearing levels between affected and healthy ears in patients with Ramsay Hunt syndrome with sensorineural hearing loss on the initial pure tone audiogram (n = 9, except case 1 with deafness). Their hearing recovered to normal range or the same level as the unaffected ear, except in case 1 with deafness (not shown) and cases 2 and 3 (■, ○) with moderate hearing loss. Case 4, • case 5, –; case 6, *; case 7, x; case 8, ▲; case 13, –; case 14, +.

RIGHTSLINK

Acta Otolaryngol Downloaded from informahealthcare.com by (D)Tokushima U Kuramoto on 02/04/14
For personal use only.

(%) = 100 – (amplitude on the affected side)/(amplitude on the healthy side) × 100.

For the caloric test, cold-water (15°C, 5 ml) irrigation was used and caloric nystagmus was recorded by electronystagmography. The maximum slow-phase eye velocity was measured and the caloric response was calculated by addition or subtraction of the averaged slow-phase eye velocity of spontaneous nystagmus. A caloric response of less than 20°/s was determined as CP.

Patients were then scanned on a 1.5 T MR unit (Signa1.5THDxt, GE) to obtain three-dimensional T1-weighted fast field-echo images at 25.4 ± 15.8 days after the onset. The imaging parameters were as follows: repetition time 10.5 ms, echo time 3.2 ms, flip angle 20°, 1 mm slice thickness, 200 mm field of view, and 256 × 224 (512 reconstruction) matrix. The contrast medium (Gd-DTPA) was administered intravenously at a dose of 0.1 nmol/kg. Then, images perpendicular to the IAC were reconstructed to identify the facial, superior, and inferior vestibular nerves and the cochlear nerves separately. The MRIs were evaluated by two radiologists independently without knowledge of the clinical data. The presence of abnormal contrast enhancement of the facial nerve, superior and inferior vestibular nerve, and cochlear nerve in the IAC was assessed on the basis of visual inspection of the precontrast and postcontrast images.

Fisher's exact probability test was used for statistical analysis and $p < 0.05$ was considered significant.

Results

Twelve patients with Ramsay Hunt syndrome with vertigo all showed CP on the caloric test. Eleven of them showed enhancement of the superior vestibular nerve in the IAC on Gd-enhanced MRI. Thus, there was a significant association between vertigo with CP and enhancement of the superior vestibular nerve in Ramsay Hunt syndrome patients with vertigo ($p < 0.01$) (Table I). A patient with vertigo (case 1) showed the enhancement of both superior and inferior vestibular nerves in the IAC on MRI. Vertigo and/or dizziness disappeared in nine patients, but residual dizziness continued in three patients (cases 1, 2, and 3).

Ten patients with Ramsay Hunt syndrome showed sensorineural hearing loss: profound in one, moderate in three, and mild high-frequency hearing loss in six. Figure 1 shows the differences in hearing levels between the affected and healthy ears at each patient's first visit. Three patients, case 1 with profound and cases 2 and 3 with moderate sensorineural hearing losses, showed enhanced cochlear nerves in the IAC on Gd-enhanced MRI (Table I) and their hearing loss was irreversible. By contrast, moderate hearing loss in case 13 and mild high-frequency hearing loss in six patients with no cochlear nerve enhancement on MRI recovered completely within 2 months after the onset.

All 14 patients with Ramsay Hunt syndrome showed facial palsy ranging from HB grade IV to grade VI. Only four of eight patients with total facial palsy (HB grade VI) showed enhancement of the facial nerve in the IAC on Gd-enhanced MRI (Table I). The facial palsy recovered to HB grade I in two, and one patient each to grade II and III. In the remaining 10 patients with no enhancement of the facial nerve on MRI, facial palsy recovered to HB grade I in eight, grade II in one, and grade III in one patient.

Case 1 showed Gd enhancement of all four nerves: facial, superior, and inferior vestibular nerves and cochlear nerves in the IAC on MRI (Figure 2a). Although her facial palsy recovered to HB grade III and vertigo disappeared, residual dizziness and profound sensorineural hearing loss continued a year after the onset. Case 2 and case 3 (Figure 2b) showed Gd enhancement of three nerves – facial, superior vestibular, and cochlear nerves in the IAC on MRI. Although their facial palsy recovered to HB grade I and II, respectively, and vertigo disappeared, residual dizziness and moderate sensorineural hearing loss continued a year after the onset.

Case 4 showed Gd enhancement of two nerves, the facial and superior vestibular nerves in the IAC on MRI (Figure 2c). Her facial palsy recovered completely, and vertigo/dizziness and hearing loss disappeared within 2 months after the onset. Seven patients including case 8 (Figure 2d) showed Gd enhancement of the superior vestibular nerve only. Their facial palsy recovered and vertigo/dizziness disappeared. Three patients showed no Gd enhancement of any seventh and eighth cranial nerves in the IAC on MRI, with the recovery of their facial palsy, and the disappearance of their vertigo/dizziness and/or hearing loss.

Discussion

In the present study, 12 patients with Ramsay Hunt syndrome with vertigo all showed CP in the caloric test. Such a high frequency of CP on the caloric test was also reported previously in patients with Ramsay Hunt syndrome [4,5]. All except one patient showed the enhancement of the superior vestibular nerve in the IAC on Gd-enhanced MRI. Thus, there was a significant association between vertigo with CP and enhancement of the superior vestibular nerve in Ramsay Hunt syndrome patients. Since the caloric test primarily stimulates the lateral semicircular canal, it can be used to assess the superior vestibular nerve, which innervates the lateral and anterior semicircular

RIGHTSLINK

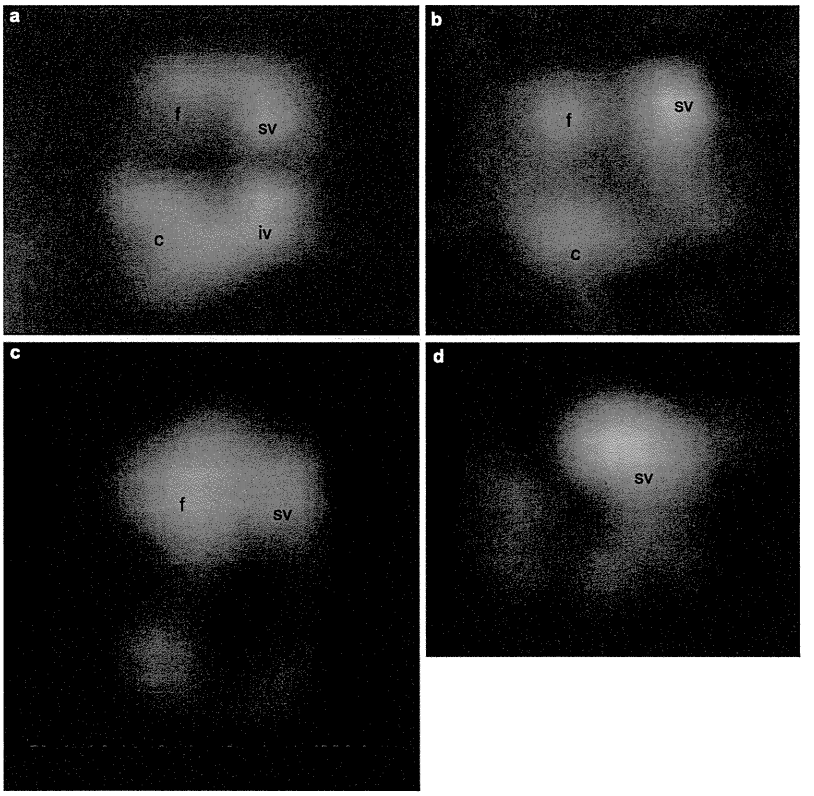

Figure 2. (a) Case 1: facial palsy of HB grade VI, CP, and deafness. The patient had residual dizziness and deafness that continued a year after the onset. Facial (f), superior (sv), and inferior vestibular (iv), and cochlear (c) nerves were enhanced by Gd in the internal auditory canal (IAC) on MRI. (b) Case 3: facial palsy of HB grade VI, CP, and flat type of mild sensorineural hearing loss (◇ in Figure 1). The patient had residual dizziness and moderate sensorineural hearing loss that continued a year after the onset. f, sv, and c nerves were enhanced by Gd in the IAC on MRI. (c) Case 4: facial palsy of HB grade VI, CP, and mild high-frequency sensorineural hearing loss (• in Figure 1). Her facial palsy fully recovered, and vertigo/dizziness and hearing loss disappeared within 2 months of the onset. f and sv nerves were enhanced by Gd in the IAC on MRI. (d) Case 8: facial palsy of HB grade IV, CP, and mild high-frequency sensorineural hearing loss (▲; in Figure 1). Her facial palsy fully recovered, and vertigo/dizziness and hearing loss disappeared within 2 months of the onset. Only the sv nerve was enhanced by Gd in the IAC on MRI.

canals and utricle. Therefore, it is suggested that the origin of vertigo in patients with Ramsay Hunt syndrome is the lesion of the superior vestibular nerve. Moreover, both superior and inferior vestibular nerves were enhanced in case 1, who showed vertigo. A previous study reported the disappearance of caloric response and vestibular evoked myogenic response (VEMP) in dizzy patients with Ramsay Hunt syndrome [5]. Taken together, the above observation also suggested that in some cases lesions to both superior and inferior vestibular nerves induce vertigo, because the inferior vestibular nerve innervates the saccule that is the origin of VEMP. There is another possibility that the lesion of the superior vestibular nerve induces vertigo and affects VEMP, because the superior vestibular nerve innervates the anterosuperior part of the sacculus in addition to the lateral and anterior semicircular canals and the utricle.

Gd does not normally cross the blood–nerve barrier. However, it is postulated that inflammation induced by reactivated VZV breaks down the blood–nerve barrier and increases the permeability of Gd from the blood to the nerve [3]. This is the possible mechanism of Gd enhancement of the affected facial nerve on MRI. Since the facial nerve is connected to the superior vestibular nerve by the faciovestibular anastomosis [6], Gd enhancement of the superior vestibular nerve on MRI in Ramsay Hunt syndrome patients with vertigo suggests superior vestibular neuritis due to reactivated VZV from the geniculate ganglion through the anastomosis. Subsequently, the adjoining inferior vestibular nerve may be infected by VZV. However, the superior nerve is more susceptible to inflammation than the inferior nerve, because the lateral bony channel of the superior vestibular nerve is longer and contains more bony spicules [7].

Acta Otolaryngol Downloaded from informahealthcare.com by (D)Tokushima U Kuramoto on 02/04/14
For personal use only.

RIGHTSLINK

Acta Otolaryngol Downloaded from informahealthcare.com by (D)Tokushima U Kuramoto on 02/04/14
For personal use only.

Seven of the 10 Ramsay Hunt syndrome patients with sensorineural hearing loss who showed no enhancement of the cochlear nerve had a complete recovery and their right–left differences in hearing loss were mostly mild and limited to high frequencies. This finding is in line with a previous report that showed a good prognosis of sensorineural hearing loss that mainly affected high frequencies in patients with Ramsay Hunt syndrome [8,9]. In the remaining three patients with Gd enhancement of the cochlear nerve in the IAC, profound hearing loss in case 1 and moderate hearing loss in cases 2 and 3 were irreversible. The close association between the enhancement of the cochlear nerve and refractory hearing loss in patients with Ramsay Hunt syndrome suggests that the origin of refractory sensorineural hearing loss might be the cochlear neuritis. Therefore, moderate hearing loss in case 13 recovered completely, probably because his cochlear nerve was not enhanced in MRI. Retrocochlear involvement in patients with Ramsay Hunt syndrome has also been reported [4,9]. Since the cochlear nerve is connected to the inferior vestibular nerve by the Oort's anastomosis [6], reactivated VZV from the geniculate ganglion may spread to the vestibular and cochlear nerves through the faciovestibular and Oort's anastomoses, as seen in case 1 who showed Gd enhancement of the superior and inferior vestibular nerves and the cochlear nerve in the IAC on MRI. However, the mechanisms of moderate hearing loss in cases 2 and 3 with enhancement of cochlear nerve and mild hearing loss in other patients who show no enhancement of cochlear nerve are unknown.

A previous report has shown Gd enhancement of the facial nerve in the IAC and the geniculate ganglion a week after the onset of facial palsy in patients with herpetic facial palsy, suggesting that the peak of inflammatory response to VZV occurs at around 10–14 days after the onset [10,11]. In contrast, in the present study, Gd enhancement of the facial nerve in the IAC was observed in only four patients with Ramsay Hunt syndrome on MRI obtained more than 20 days after the onset of the palsy. In addition, there was no correlation between Gd enhancement of facial nerve in the IAC on MRI and the prognosis of facial palsy in patients with Ramsay Hunt syndrome, which is in line with previous studies [3,12].

In conclusion, our data demonstrate that vertigo in patients with Ramsay Hunt syndrome is mostly induced by superior vestibular neuritis infected by reactivated VZV from the geniculate ganglion through the faciovestibular anastomosis, as demonstrated in all except one dizzy patient with Ramsay Hunt syndrome, showing both CP on the caloric test and Gd enhancement of the superior vestibular nerve in the IAC on MRI. Refractory hearing loss in patients with Ramsay Hunt syndrome may be due to cochlear neuritis involved in the spread of VZV, as shown in three patients with severe or moderate sensorineural hearing loss and Gd enhancement of the cochlear nerve in the IAC on MRI. Further studies including a quantitative analysis of enhancement on MRI are needed to prove the above hypothesis.

Acknowledgment

This work was financially supported by Grant-in-Aid from the Ministry of Health and Welfare of Japan.

Declaration of interest: The authors report no conflicts of interest. The authors alone are responsible for the content and writing of the paper.

References

[1] Sweeney CJ, Gilden DH. Ramsay Hunt syndrome. J Neurol Neurosurg Psychiatry 2001;71:149–54.
[2] Wackym PA. Molecular temporal bone pathology: II. Ramsay Hunt syndrome (herpes zoster oticus). Laryngoscope 1997;107:1165–75.
[3] Jonsson L, Tien R, Engström M, Thuomas KA. Gd--DPTA enhanced MRI in Bell's palsy and herpes zoster oticus: an overview and implications for future studies. Acta Otolaryngol 1995;115:577–84.
[4] Kaberos A, Balatsouras DG, Korres SG, Kandiloros D, Economou C. Audiological assessment in Ramsay Hunt syndrome. Ann Otol Rhinol Laryngol 2002;111:68–76.
[5] Lu YC, Young YH. Vertigo from herpes zoster oticus: superior or inferior vestibular nerve origin? Laryngoscope 2003; 113:307–11.
[6] OzdoĞmuş O, Sezen O, Kubilay U, Saka E, Duman U, San T, et al. Connections between the facial, vestibular and cochlear nerve bundles within the internal auditory canal. J Anat 2004;205:65–75.
[7] Gianoli G, Goebel J, Mowry S, Poomipannit P. Anatomic differences in the lateral vestibular nerve channels and their implications in vestibular neuritis. Otol Neurotol 2005;26: 489–94.
[8] Wayman DM, Pham HN, Byl FM, Adour KK. Audiological manifestations of Ramsay Hunt syndrome. J Laryngol Otol 1990;104:104–8.
[9] Abramovich S, Prasher DK. Electrocochleography and brain-stem potentials in Ramsay Hunt syndrome. Arch Otolaryngol Head Neck Surg 1986;112:925–8.
[10] Suzuki F, Furuta Y, Ohtani F, Fukuda S, Inuyama Y. Herpes virus reactivation and gadolinium-enhanced magnetic resonance imaging in patients with facial palsy. Otol Neurotol 2001;22:549–53.
[11] Korzec K, Sobol SM, Kubal W, Mester SJ, Winzelberg G, May M. Gadolinium-enhanced magnetic resonance imaging of the facial nerve in herpes zoster oticus and Bell's palsy: clinical implications. Am J Otol 1991;12:163–8.
[12] Brändle P, Satoretti-Schefer S, Böhmer A, Wichmann W, Fisch U. Correlation of MRI, clinical, and electroneurongraphic findings in acute facial nerve palsy. Am J Otol 1996; 17:154–61.

RIGHTSLINK

Acta Oto-Laryngologica. 2013; 133: 1292–1296

informa
healthcare

ORIGINAL ARTICLE

Effects of endolymphatic sac decompression surgery on endolymphatic hydrops

MUNEHISA FUKUSHIMA, TADASHI KITAHARA, ARATA HORII & HIDENORI INOHARA

[1]*Department of Otolaryngology, Osaka University, Graduate School of Medicine, Oskaka, Japan*

Acta Otolaryngol Downloaded from informahealthcare.com by Osaka University on 11/19/13
For personal use only.

Abstract

Conclusions: The present findings suggest that complete control of vertigo after endolymphatic sac decompression surgery (ESDS) does not always depend on improved vestibular function or reduced endolymphatic hydrops. Vertigo control is, however, associated with hearing stability.

Objective: Among surgical treatments for intractable Meniere's disease, ESDS is performed to preserve and improve inner ear function. We examined the correlation between changes in vertigo frequency and neuro-otologic function to understand the condition of the inner ear in patients whose vertigo was completely controlled after undergoing ESDS.

Methods: This was a retrospective cross-tabulation study. Between 1997 and 2001, we treated 52 patients with intractable vertigo using ESDS and followed the patients regularly for 2 years. Postoperatively we evaluated and recorded changes in vertigo attack frequency, maximum slow phase eye velocity, worst hearing level, and glycerol test results according to modified American Academy of Otolaryngology–Head and Neck Surgery 1995 criteria.

Results: We found no correlation between vertigo control and vestibular function. There was also no correlation between vertigo control and negative conversion of the glycerol test. There was a significant correlation between vertigo control and hearing control .

Keywords: *Intractable Meniere's disease, endolymphatic sac drainage, surgical results, vertigo control*

Introduction

Meniere's disease, characterized by recurrent vertigo, fluctuating hearing loss, tinnitus, and aural fullness, is a common disease with an incidence of 17–46 cases per 100 000 population [1]. Despite the use of various medications, some of those patients are frequently prevented from participating in activities of daily life owing to frequent vertigo attacks and progressive sensorineural hearing loss. Patients with these severe symptoms are said to have intractable Meniere's disease.

When conservative medical treatment has failed, surgical strategies such as endolymphatic sac decompression surgery (ESDS), vestibular neurectomy, and labyrinthectomy are considered depending on the conditions in each patient. ESDS, first performed by Portmann in 1927 [2], is still commonly used worldwide. One reason for its reputation as a mainstay surgical treatment for intractable Meniere's disease is that – unlike other, ablative procedures – ESDS is nondestructive. Its purpose is to preserve and improve inner ear function.

Temporal bone studies in 1938 revealed that the otopathology of Meniere's disease is endolymphatic hydrops [3,4]. ESDS drains the excessive endolymph and decompresses membranous labyrinthine pressure. It has been reported that ESDS accomplishes complete vertigo control in 42–88% of patients [5–10]. To date, no evidence has been presented that elucidates the mechanisms that produce the symptomatic relief resulting from shunting or decompressing the endolymphatic sac. Does ESDS improve inner ear function, resulting in good vertigo results? Alternatively, is

Correspondence: Tadashi Kitahara MD PhD, Department of Otolaryngology, Osaka University, Graduate School of Medicine, 2-2 Yamada-oka, Suita-city, Osaka 565-0871, Japan. Tel: +81 6 6879-3951. Fax: +81 6 6879 3959. E-mail: tkitahara@ent.med.osaka-u.ac.jp

(Received 3 July 2013; accepted 30 July 2013)

ISSN 0001-6489 print/ISSN 1651-2251 online © 2013 Informa Healthcare
DOI: 10.3109/00016489.2013.831480

RIGHTSLINK

it no more effective than a placebo operation [11]? To understand the inner ear conditions in patients for whom ESDS provided complete vertigo control, we examined the correlation between changes in vertigo frequency and neuro-otologic function.

Material and methods

Patients

The Ethics Committee of Osaka University Hospital approved this study (certificate no. 0421). The study is registered with ClinicalTrials.gov of the US Food and Drug Administration (certificate no. NCT00500474).

A total of 52 patients with a clinical diagnosis of Meniere's disease according to the 1995 American Academy of Otolaryngology–Head and Neck Surgery (AAO-HNS) criteria were eligible for enrollment in the study [12]. Intractable Meniere's disease was designated in cases where at least 6 months of various forms of medical and psychological management had been applied and had failed [1]. Between 1997 and 2001, we performed ESDS on 52 patients (19 men and 33 women; 42 unilateral and 10 bilateral) with a mean age of 47.1 ± 15.9 years (range 23–80 years). The duration of disease was a mean of 60.4 ± 8.9 months (range 6–256 months). The surgery was performed at Osaka Rosai and Osaka University Hospitals. Postoperatively, the patients were followed regularly for at least 2 years.

Treatment

The technical details of ESDS are as follows [10]. Simple mastoidectomy was performed, clearly exposing the endolymphatic sac in the area between the sigmoid sinus and the inferior margin of the posterior semicircular canal. If possible, the sac was exposed to include the rugose portion. It was opened with an L-shaped incision made along the posterior and distal margins of the lateral wall. It was then filled with 20 mg of prednisolone. While it was dissolving, we prepared a bundle of absorbable gelatin film with fan- and stick-shaped ends. These films were tied to each other with biochemical adhesive at the stick-shaped end. The fan-shaped end was then inserted into the sac. Small pieces of absorbable gelatin sponge soaked in a high concentration of dexamethasone (32 mg/4 ml) were placed inside and outside the sac lumen, which expanded with the bundle. The dexamethasone-containing sponges placed outside the sac were coated with the adhesive so dexamethasone was slowly delivered into the sac over a long period of time. The sponges comprised a natural sustained-release vehicle. The stick-shaped end extending out of the sac was fixed to the front edge of the mastoid cavity with the same adhesive so the incision into the sac remained expanded for as long as possible. The mastoid cavity was filled with relatively large pieces of absorbable gelatin sponge dipped in a steroid–antibiotic solution, after which the wound was closed with skin sutures.

Functional examinations

A definitive dizzy spell lasting more than 20 min was regarded as a Meniere's vertigo attack according to the modified 1995 AAO-HNS criteria [12]. The frequency of vertigo was calculated based on the number of vertigo attacks during the 6 months before surgery. Frequency after surgery was calculated based on the number of vertigo attacks during the 6 months between 18 and 24 months after surgery. The data could be obtained for all the 52 cases.

Vestibular function was measured by a caloric test using electronystagmography (ENG) twice, during the 6 months before surgery and during the 6 months between 18 and 24 months after surgery. For the test, the external auditory canal was irrigated, in turn, with 30°C cold water and 44°C hot water (20 ml) for 10 s each. The induced nystagmus was recorded using ENG in a dark, open-eyes situation. Based on the mean maximum slow-phase eye velocity (max-SPEV) on the treated side, the max-SPEVafter treatment/max-SPEV before treatment ratio was calculated. Values > 1.1 were recognized as an improvement in vestibular function during the second follow-up year [10]. It is not easy to evaluate vestibular improvement using changes in caloric responses. Using the furosemide test criteria to detect vestibular endolymphatic hydrops, changes of ± 10% were considered positive [13]. The data could be obtained from 50 of 52 cases, because of the lack of paired examinations in two cases.

Hearing function was measured by a pure-tone audiometer and was evaluated based on the four-tone average formulated by (a + b + c + d)/4 (a, b, c, d are hearing levels at 0.25, 0.5, 1.0, and 2.0 kHz, respectively) according to the modified 1995 AAO-HNS criteria [12]. The worst hearing level during the 6 months before surgery was adopted as the hearing level before treatment ('before'). The worst hearing level during the 6 months between 18 and 24 months after surgery was adopted as the hearing level at the second follow-up year ('after'). Differences in hearing levels > 10 dB before and after treatment were regarded as 'better.' Differences smaller than –10 dB were regarded as

Acta Otolaryngol Downloaded from informahealthcare.com by Osaka University on 11/19/13
For personal use only.

RIGHTSLINK